

University of Dundee

E3 ubiquitin ligases LNX1 and LNX2 localize at neuronal gap junctions formed by connexin36 in rodent brain and molecularly interact with connexin36

Lynn, Bruce D.; Li, Xinbo; Hormuzdi, Sheriar G.; Griffiths, Emily K.; McGlade, C. Jane; Nagy, James I.

Published in:
European Journal of Neuroscience

DOI:
[10.1111/ejn.14198](https://doi.org/10.1111/ejn.14198)

Publication date:
2018

Document Version
Peer reviewed version

[Link to publication in Discovery Research Portal](#)

Citation for published version (APA):

Lynn, B. D., Li, X., Hormuzdi, S. G., Griffiths, E. K., McGlade, C. J., & Nagy, J. I. (2018). E3 ubiquitin ligases LNX1 and LNX2 localize at neuronal gap junctions formed by connexin36 in rodent brain and molecularly interact with connexin36. *European Journal of Neuroscience*, 48(9), 3062-3081.
<https://doi.org/10.1111/ejn.14198>

General rights

Copyright and moral rights for the publications made accessible in Discovery Research Portal are retained by the authors and/or other copyright owners and it is a condition of accessing publications that users recognise and abide by the legal requirements associated with these rights.

- Users may download and print one copy of any publication from Discovery Research Portal for the purpose of private study or research.
- You may not further distribute the material or use it for any profit-making activity or commercial gain.
- You may freely distribute the URL identifying the publication in the public portal.

Take down policy

If you believe that this document breaches copyright please contact us providing details, and we will remove access to the work immediately and investigate your claim.

DR. JAMES I NAGY (Orcid ID : 0000-0003-2753-091X)

Article type : Research Report

Associate Editor: Dr. Masahiko Watanabe; Section: Molecular & Synaptic Mechanisms

E3 ubiquitin ligases LNX1 and LNX2 localize at neuronal gap junctions formed by connexin36 in rodent brain and molecularly interact with connexin36

B. D. Lynn^{1*}, Xinbo Li^{2*}, S. G. Hormuzdi³, E. K. Griffiths⁴, C. J. McGlade⁴ and J. I. Nagy^{1}**

¹Department of Physiology and Pathophysiology, Max Rady College of Medicine, Rady Faculty of Health Science, University of Manitoba, Winnipeg, Canada

²Casey Eye Institute, Oregon Health and Science University, Portland, Oregon, USA

³Division of Neuroscience, Ninewells Hospital and Medical School, University of Dundee, Dundee DD1 9SY, UK.

⁴Department of Medical Biophysics, University of Toronto, Toronto, Canada, and Arthur and Sonia Labatt Brain Tumour Research Centre, Hospital for Sick Children, Toronto, Canada

Running title: E3 ubiquitin ligases and connexin36

Keywords: gap junctions, electrical synapses, ubiquitination, connexin degradation, connexin trafficking.

*Contributed equally as first co-authors

**Address for correspondence

Dr. James I. Nagy

Department of Physiology and Pathophysiology

Max Rady College of Medicine, University of Manitoba

This is the peer reviewed version of the following article: Lynn, B.D., et al. 'E3 ubiquitin ligases LNX1 and LNX2 localize at neuronal gap junctions formed by connexin36 in rodent brain and molecularly interact with connexin36', *European Journal of Neuroscience* (2018) which has been published in final form at <https://doi.org/10.1111/ejn.14198>. This article may be used for non-commercial purposes in accordance with Wiley Terms and Conditions for Self-Archiving. This article is protected by copyright. All rights reserved.

745 Bannatyne Ave, Winnipeg, Manitoba, Canada R3E 0J9

Email: James.Nagy@umanitoba.ca

Tel. (204) 789-3767, Fax (204) 789-3934

Abstract

Electrical synapses in the mammalian central nervous system (CNS) are increasingly recognized as highly complex structures for mediation of neuronal communication, both with respect to their capacity for dynamic short and long-term modification in efficacy of synaptic transmission and their multi-molecular regulatory and structural components. These two characteristics are inextricably linked, such that understanding of mechanisms that contribute to electrical synaptic plasticity requires knowledge of the molecular composition of electrical synapses and the functions of proteins associated with these synapses. Here, we provide evidence that the key component of gap junctions that form the majority of electrical synapses in the mammalian CNS, namely connexin36 (Cx36), directly interacts with the related E3 ubiquitin ligase proteins Ligand of NUMB protein X1 (LNX1) and Ligand of NUMB protein X2 (LNX2). This is based on immunofluorescence co-localization of LNX1 and LNX2 with Cx36-containing gap junctions in adult mouse brain *vs.* lack of such co-association in LNX null mice, co-immunoprecipitation of LNX proteins with Cx36, and pull-down of Cx36 with the second PDZ domain of LNX1 and LNX2. Further, co-transfection of cultured cells with Cx36 and E3 ubiquitin ligase-competent LNX1 and LNX2 isoforms led to loss of Cx36-containing gap junctions between cells, whereas these junctions persisted following transfection with isoforms of these proteins that lack ligase activity. Our results suggest that a LNX protein mediates ubiquitination of Cx36 at neuronal gap junctions, with consequent Cx36 internalization, and may thereby contribute to intracellular mechanisms that govern the recently identified modifiability of synaptic transmission at electrical synapses.

Introduction

Gap junctions formed between apposing cells by various members of the family of twenty connexin proteins mediate gap junctional intercellular communication, where junctional channels allow cell-to-cell passage of ions and small molecules (Goodenough & Paul, 2009). Such junctions between neurons in the central nervous system (CNS) provide for direct electrical neuronal communication and are the morphological basis of electrical synapses (Bennett, 1997; Bennett & Zukin, 2004). In the mammalian CNS, neuronal gap junctions

formed by connexin36 (Cx36) are widely distributed (Condorelli *et al.*, 2000; Nagy *et al.*, 2018), and have critically important functions in establishing synaptic circuitry during development (Miller & Pereda, 2017) and in facilitating synchronous neuronal activity in mature brain (Hormuzdi *et al.*, 2004; Connors, 2009). It has recently been recognized that electrical synapses are highly dynamic, with reports indicating that neuronal communication mediated by these synapses is subject to modification by a variety of processes. These include regulation of electrical coupling by various neurotransmitters (Nagy *et al.*, 2018), by the state of neuronal activity (Haas *et al.*, 2011), by connexin phosphorylation (Urschel *et al.*, 2006; Kothmann *et al.*, 2009; O'Brien, 2014) and by ion-mediated gating of Cx36-containing channels (Palacios-Prado *et al.*, 2013, 2014). Importantly, such regulation has a functional impact on the behaviour of neuronal networks interconnected by electrical synapses in neural circuitry (Bloomfield & Volgyi, 2009; Pereda *et al.*, 2013; Pereda, 2014; Haas *et al.*, 2016; Curti & O'Brien, 2016).

The exact mechanisms underlying modulation of the strength of electrical coupling are not fully understood, but one possibility is via regulated trafficking of Cx36 into and out of gap junctions via exocytosis and endocytosis of Cx36 channels (Pereda *et al.*, 2013; Pereda, 2014). Such trafficking has been documented at vertebrate electrical synapses, and interference with this process rapidly altered electrical coupling (Flores *et al.*, 2012), which is consistent with the high turnover rate of Cx36, estimated to be ~1-3 hr (Flores *et al.*, 2012; Wang *et al.*, 2015) and is similar to that of other connexins (Evans & Martin, 2002; Berthoud *et al.*, 2004). Such trafficking presumably occurs via processes governing Cx36 removal and disposal, which for most connexins are poorly understood, with the exception of connexin43 (Cx43) that undergoes ubiquitination and degradation by the proteasome pathway (Berthoud *et al.*, 2004; Kjenseth *et al.*, 2010; Herve *et al.*, 2012). The attachment of ubiquitin to target proteins is a common cellular sorting mechanism for determination of protein fate along the endocytotic and exocytotic pathways (Deshaies & Joazeiro, 2009). Ubiquitination involves the covalent linkage of ubiquitin to lysine residues of target proteins. This process occurs via a stepwise enzyme cascade that requires three distinct enzyme participants; a ubiquitin-activating enzyme (E1), a ubiquitin-conjugating enzyme (E2) and a ubiquitin-ligase (E3). The E3 ligase in this cascade determines target-protein specificity, and over 600 E3 ligases have been identified and distinguished by characteristics of their catalytic domain, which include the HECT, RING and U-box family of proteins (Bhoj and Chen, 2009). Many RING domain E3 ligases contain additional domains required for their specific interaction with target

proteins, including PDZ (PSD-95, DlgA, ZO-1) domains that mediate interaction with the PDZ ligand of their target proteins (Ye & Zhang, 2013).

We previously reported that Cx36 contains a PDZ domain interaction motif, consisting of a SAYV amino acid sequence at its carboxy-terminus, that mediates its interaction with the PDZ domains of various proteins, including the first PDZ domains of zonula occludens (ZO) proteins ZO-1, ZO-2, ZO-3, the tenth PDZ domain of multi-PDZ domain protein1 (MUPP1) and the single PDZ domain in AF6 (aka, afadin) (Li *et al.*, 2004a,b, 2009, 2012). This carboxy-terminus SAYV PDZ ligand is contained in other proteins (*e.g.*, claudin-1 and CD8 α), where it mediates protein-protein interaction for ubiquitination by specific E3-ubiquitin ligases, namely, Ligand of NUMB protein X1 (LNX1) and Ligand of NUMB protein X2 (LNX2) (Takahashi *et al.*, 2009; D'Agostino *et al.*, 2011). This raised the possibility of Cx36 interaction with LNX1 and/or LNX2. These two related proteins are RING domain E2-dependent E3 ubiquitin ligases whose PDZ domains are required for mediation of interactions with proteins targeted for ubiquitination. They share identical domain structure comprised of one amino-terminal RING domain and four PDZ domains (Rice *et al.*, 2001). Each of the four PDZ domains of LNX1 and LNX2 interact with specific classes of PDZ ligands (Wolting *et al.*, 2011; Lenihan *et al.*, 2017a). LNX2 is expressed in many tissues, including adult brain (Rice *et al.*, 2001; Lenihan *et al.*, 2014). More complex is LNX1, where three protein isoforms have been identified; a full-length form containing the RING finger catalytic domain (LNX1p80), an alternatively spliced form devoid of this domain and thus lacking catalytic activity (LNX1p70), and a novel recently characterized LNX1p62 brain isoform also lacking the catalytic domain (Dho *et al.*, 1998; Xie *et al.*, 2001; Lenihan *et al.*, 2014). In brain, LNX1p80 appears to be absent, whereas catalytically inactive LNX1p70 is expressed mainly in neurons and in a small subset of oligodendrocytes (Dho *et al.*, 2001; Lenihan *et al.*, 2014).

In order to explore means whereby Cx36 deployment, trafficking and degradation could contribute to the plasticity of electrical synapses, we investigated Cx36 relationships with LNX1 and LNX2. We examined immunofluorescence localization of these proteins in combination with immunolabelling for Cx36, and used molecular and biochemical approaches to assess Cx36/LNX interaction.

Materials and methods

Animals and antibodies

Animals were utilized according to approved protocols by the Central Animal Care Committee of the University of Manitoba and by the Hospital for Sick Children Animal Care and Use Committee, with minimization of the numbers animals used. A total of four Sprague-Dawley rats and eight wild-type C57BL/6 mice used in this study were obtained from Central Animal Care Services at the University of Manitoba. In addition, the two C57BL/6 LNX1 knockout (KO) mice used were obtained from the Toronto Centre for Phenogenomics. Brains from these animals were prepared and taken for immunofluorescence labelling and immunoblotting as described below. The LNX1 gene ablated mutant mouse strain was generated in the laboratory of Dr. Mark Henkemeyer (University of Texas Southwestern) as described (Liu *et al.*, submitted). Briefly, LNX1 was targeted by homologous recombination in the R1 ES cell line, germline transmission was obtained by aggregation chimeras, and the LNX1 KO mice obtained were backcrossed to C57BL/6 mice for multiple generations and were bred and maintained under institute guidelines at the Toronto Centre for Phenogenomics.

Antibodies used included a mouse monoclonal anti-Cx36 (Cat. No. 39-4200) and a rabbit polyclonal anti-Cx36 (Cat. No. 51-6300), which were obtained from ThermoFisher (ThermoFisher, Rockford, IL, USA) and used at a concentration of 2-3 µg/ml. In addition, rabbit polyclonal anti-LNX1 and LNX2 antibodies were obtained originally from Invitrogen (Invitrogen, Carlsbad, CA, USA), before this provider was acquired by Life Technologies and then ThermoFisher. Two anti-LNX1 antibodies were generated against peptide sequences corresponding to amino acids 200-213 and 247-259 in LNX1, designated ab200 and ab247, and one anti-LNX2 antibody was generated against a peptide corresponding to amino acid sequence 442-458 in LNX2, designated ab442. Additional rabbit polyclonal anti-LNX1 antibody, used for immunoblotting of LNX1 from mouse tissues and for co-IP of Cx36 with LNX1 from mouse brain, were generated against GST fusion proteins containing LNX1 amino acids (aa) 8-210 and aa365-478, designated ab8 and ab365, respectively (Dho *et al.*, 1998). All antibodies against LNX were used at a dilution of 1:250. Mouse monoclonal anti-His 6X-tag (Cat. No. R930) and a monoclonal rabbit anti-eGFP (enhanced green fluorescent protein) (Cat No. G10362) were obtained from ThermoFisher and both were used at a concentration of 2 µg/ml, a mouse monoclonal anti-FLAG (M2) antibody (Cat. No. F1804)

was obtained from Millipore Sigma (Sigma-Aldrich Corp., St. Louis, MO, USA) and used at a dilution of 1:1000. Mouse monoclonal anti-HA tag (F-7) antibody (Cat. No. 7392) was obtained from Santa Cruz (Santa Cruz Biotechnology, Dallas TX, USA) and used at a concentration of 2 µg/ml.

Immunofluorescence procedures

Procedures used here for preparation of tissue for immunofluorescence have been previously described in detail for immunolabelling of Cx36 in combination with other proteins (Li *et al.*, 2012; Lynn *et al.*, 2012; Rubio & Nagy; 2015). Briefly, animals were first euthanized with an intraperitoneal injection of equithesin (3 ml per kg) and then transcardially perfused sequentially with a pre-fixative solution followed by a fixative solution containing buffered 1% formaldehyde/0.2% picric acid. Cryostat sections were collected at a thickness of 15 µm and immunolabelled with monoclonal anti-Cx36. For double immunofluorescence labelling, sections were simultaneously incubated with two primary antibodies (a mouse monoclonal and a rabbit polyclonal: Cx36 + LNX1; Cx36 + LNX2) in a dilution buffer containing 50 mM Tris-HCl, pH 7.4, containing 1.5% sodium chloride and 0.3% Triton X-100 (TBSTr) supplemented with 5% normal goat or normal donkey serum. Following incubation for 24 hr at 4°C, the sections were washed for 1 h in TBSTr, and then incubated for 1.5 h at room temperature simultaneously with appropriate combinations of secondary antibodies diluted in TBSTr with normal goat or donkey serum. Secondary antibodies included Cy3-conjugated goat anti-mouse IgG diluted 1:500 (Jackson ImmunoResearch Laboratories, West Grove, PA, USA) and Alexa Fluor 488-conjugated goat anti-rabbit IgG diluted 1:1000 (Molecular Probes, Eugene, Oregon). After secondary antibody incubations, sections were washed in TBSTr for 20 min, then in 50 mM Tris-HCl buffer, pH 7.4 for 30 min, covered with antifade medium and coverslipped. Control procedures included omission of one of the primary antibodies with inclusion of each of the secondary antibodies to establish the absence of inappropriate cross-reactions between primary and secondary antibodies.

Wide-field and confocal immunofluorescence microscopy were conducted on a Zeiss Axioskop2 fluorescence microscope (Carl Zeiss Canada, Toronto, Ontario, Canada) and on a Zeiss LSM 710 confocal microscope using ZEN software (Olympus Canada, Inc., Markham, ON, Canada), respectively. Figure plates were assembled using Adobe Photoshop CS (Adobe Systems, San Jose, CA, USA) and CorelDraw Graphics (Corel Corporation, Ottawa, ON,

Canada). Confocal images of double labelling of Cx36 with either LNX1 or LNX2 in brain sections were acquired using an oil immersion 40x objective lens with numerical aperture of 1.4. All of the confocal images presented here were captured at a zoom factor ranging from 3.3 to 5.5 and a resolution of 1024 x 1024 pixels, and show single scans or maximum intensity projection z-stacks of 2 to 7 optical scans, with a step size of 0.43 μm (defined as optimum for a 40x objective), giving projection thicknesses ranging from 1.72 to 3.44 μm , and are displayed without deconvolution. Laser illumination intensities and photomultiplier tube gains settings were adjusted to well below saturation of the most intense labelling observed to allow capture of the full range of labelling intensities and to minimize halation which can artificially increase the size of immunofluorescent areas of interest. As we observed minimal fading of fluorescence with the laser setting chosen, the laser dwell time was increased to a moderate level to provide for better image quality. A total of 56 single and z-stack images were collected for a total of 122 images when the z-stack optical scans are considered separately, representing collectively all the brain regions examined. Before compression of the optical scans into a single image, each of the scans in a z-stack series was examined separately to exclude possible artifactual overlap of labelling for Cx36 with label for LNX that may occur from labels that were actually separated in the z-dimension. In addition, the image stacks were displayed in a 3-dimensional configuration, allowing 360 degree image rotation in the x, y and z dimensions to further confirm the label for Cx36 and LNX remained associated at all angles of rotation.

Cell culture and transfection

HeLa cells (HeLa-WT), HeLa cells stably transfected with Cx36 (HeLa-Cx36), Neuro-2A (N2A) and HEK293T cells were grown in Dulbecco's Modified Eagle's medium (DMEM) supplemented with 10% fetal bovine serum and maintained in a tissue culture incubator at 37°C with 5% CO₂. Transient transfections were conducted using Lipofectamine LTX transfection reagent according to manufacturer's instructions (Invitrogen). Expression plasmids used for transfections included previously described LNX1p80-FLAG, LNX1p70 and LNX2-FLAG (Nie *et al.*, 2002). Additionally, transfection with mutant expression plasmids included LNX1p80^{C48A}-FLAG and LNX2^{C51A}-FLAG that each contains a functionally negative mutation within the zinc coordination site of the N-terminal RING domain of LNX1p80 and LNX2, which is required for ubiquitination competence (Nie *et al.*, 2002). A HA-ubiquitin plasmid in pcDNA3.1 was a gift from Dr. E. Yeh (Addgene plasmid # 18712; Kamitani *et al.*, 1997). A full-length Cx36 plasmid and a truncated Cx36 Δ 4 plasmid

that lacks coding sequence for the last four C-terminal amino acids in Cx36 (trCx36), which constitute its PDZ domain interaction motif, were previously described (Li *et al.*, 2004a,b). C-terminal tagging of Cx36 prevents its interaction with proteins that bind the Cx36 C-terminus. Thus, in the construct we used here (provided by Dr. S. G. Hormuzdi, University of Dundee), enhanced cyan fluorescent protein (eCFP) is inserted 15 amino acids upstream of the C-terminus PDZ ligand in otherwise full-length Cx36, freeing this ligand for interaction with the PDZ domains of Cx36-interacting partners. This construct was previously shown to form functionally communicating gap junctions (Helbig *et al.*, 2010). Following cell transfection (18-20 h), cultures of cells grown on glass coverslips were washed in 50 mM sodium phosphate buffer, pH 7.4, containing 0.9% NaCl (PBS), fixed for 10 min in 2% formaldehyde in PBS, rinsed and stored at 4 °C. Immunofluorescence labelling of cells was conducted as described above for tissue sections.

Western blotting

Animals were euthanized with an intraperitoneal injection of equithesin (3 mg/kg), brains dissected, homogenized in 14 volumes of immunoprecipitation (IP) buffer (20 mM Tris-HCl, pH 8.0, 140 mM NaCl, 1% Triton X-100, 10% glycerol, 1 mM EGTA, 1.5 mM MgCl₂, 1 mM dithiothreitol, 1 mM phenylmethylsulphonyl fluoride) supplemented with a protease inhibitor cocktail (Millipore Sigma) and then briefly sonicated. For preparation of cell lysates, cultures were rinsed with PBS, lysed in ice-cold IP buffer (Li *et al.*, 2012), briefly sonicated, centrifuged and resulting supernatants used for IP, pull-down assays and directly for western blot analysis. The protein concentration in all samples was determined using a kit (BioRad Laboratories, Hercules CA). For immunoblotting, samples in loading buffer were separated by sodium dodecylsulphate polyacrylamide gel electrophoresis (SDS-PAGE), and proteins transferred to polyvinylidene difluoride membranes. Following transfer, membranes were blocked for 60 min in TBS-Tw (20 mM Tris pH 7.4, 150 mM NaCl, and 0.2% Tween-20) containing 5% skim milk powder and then incubated overnight at 4°C with primary antibody in TBS-Tw containing 1% skim milk. After washing in TBS-Tw, blots were incubated with horse radish peroxidase-conjugated secondary antibodies and reactive bands revealed by chemiluminescence (Fisher Scientific).

Co-immunoprecipitation and pull-down assays

Co-immunoprecipitation (co-IP) of proteins from brain extracts was conducted as we have previously described (Li *et al.*, 2004a, 2012). In brief, clarified brain homogenates in IP buffer were precleared with protein-A agarose beads and centrifuged. Supernatants were incubated overnight at 4 °C with anti-LNX1 ab200, followed by 1 h incubation with protein-A coated agarose beads. After centrifugation, beads were washed extensively with washing buffer (20 mM Tris-HCl, pH 8.0, 150 mM NaCl and 0.5% NP-40) and then incubated at 60 °C for 20 min in SDS-PAGE loading buffer containing 10% β -mercaptoethanol. Samples were taken for western blotting as described above. Control samples were taken through the IP procedure with exclusion of primary antibody. For IP of ubiquitinated Cx36-eCFP, cells co-transfected for 16-18 hrs with Cx36-eCFP, HA-ubiquitin and with either LNX2-FLAG, LNX2^{C51A}-FLAG or FLAG-vector were lysed in radioimmunoprecipitation buffer (RIPA; 50 mM Tris pH 8.0, 150 mM NaCl, 1.0% IGEPAL CA-630, 0.5% sodium deoxycholate; modified from Takahashi *et al.*, 2009) containing 2% SDS, protease inhibitors and 10 mM N-ethylmaleimide, and then briefly sonicated and clarified by centrifugation at 15,000 x g for 10 min. In sample aliquots containing 200 μ g total protein, the 2% SDS was brought down to 0.1% SDS using diluent RIPA buffer that lacked SDS, and samples were then precleared with protein-G magnetic beads (Dynabeads, ThermoFisher) for 1 h at 4 °C. The precleared lysates were incubated overnight at 4 °C with either 2 μ g of anti-eGFP or 2 μ g of normal rabbit IgG (Santa Cruz) and then incubated for 1.5 h with 50 μ l of protein-G magnetic beads. After extensive washing in RIPA buffer, beads were diluted with SDS-PAGE loading buffer supplemented with 10% β -mercaptoethanol and boiled for 10 min. Following separation of beads from IP material with magnetic force, IP material was electrophoresed by SDS-PAGE using 10% gels made using a TGX-Stain-Free FastCast Acrylamide kit (Bio-Rad), transferred to PVDF membranes using the semi-dry Trans-Blot-Turbo system according to manufacturer's instructions (Bio-Rad) and imaged with a Chemidoc MP imaging system (Bio-Rad). Membranes were probed with antibodies using procedures described above. IP experiments showing accumulation of ubiquitinated Cx36-eCFP in the presence of LNX2 and reduced accumulation in presence of LNX2^{C51A}-FLAG were repeated three times with similar results as shown in Figure 9A. Experiments showing effects of LNX2-FLAG or LNX2^{C51A}-FLAG on Cx35-eCFP detection or chloroquine and NH₄Cl-mediated recovery of Cx36-eCFP detection in the presence of LNX2-FLAG were repeated three times with similar results as shown in Figure 10.

For pull-down assays, a bacterially expressed GST-LNX1 fusion protein plasmid was used to investigate molecular interaction between Cx36 and LNX1. Fusion protein was prepared, and pull-downs using this fusion protein and HeLa-Cx36 cell lysates were performed as we have previously described (Li *et al.*, 2004a, 2012). To characterize interactions between Cx36 and the PDZ domains of LNX1 and LNX2, bacterial expression plasmids containing the separate His-tagged PDZ domains of LNX1 or LNX2 in the pET30A vector were utilized (a gift from Dr. R. Hall, Emory University School of Medicine, Atlanta GA, USA; Fam *et al.*, 2005). Plasmids were introduced into competent e-coli BL21 (DE3) cells and fusion protein expression was induced with 1 mM isopropyl- β -D-thiogalactopyranoside. Following bacterial cell lysis and clarification of the extract, His-tagged fusion proteins were purified from the supernatant using Ni-NTA resins according to manufacturer's instructions (Novagen, Madison, WI, USA) and used in pull-down assays as described elsewhere (Li *et al.*, 2012). Briefly, nickel beads linked to fusion proteins containing His-tagged PDZ domains 1-4 of LNX1 or PDZ domains 1,2 and 4 of LNX2 were incubated overnight with lysates of HeLa or N2A cells transfected with plasmid encoding either Cx36 or trCx36 lacking its 4 amino acid terminal PDZ ligand. The beads were washed in PBS buffer containing 1% Triton X-100 and proteins were eluted from beads by incubation for 15 min at 60 °C with SDS-PAGE sample buffer. The resulting pull-down samples were then analyzed by western blotting. Pull down assays as described above for the PDZ domains of LNX1 and LNX2 were repeated three times with similar results as shown in Figures 6 and 7.

To confirm loss of LNX1 proteins in gene targeted mice, tissue homogenates from adult LNX1 null and wild-type controls were taken for immunoblotting and immunoprecipitation. Tissues were collected and homogenized in radioimmunoprecipitation buffer. Total protein concentration of homogenates was determined, 50 μ g of protein was separated by SDS-PAGE, immunoblotted as described above, and blots were probed with anti-LNX1 ab8 antibody. Immunoprecipitation of LNX1 from tissue homogenates was conducted using anti-LNX1 ab365 antibody or normal rabbit IgG. Immunoprecipitates were immunoblotted and probed with anti-LNX1 ab8.

Results

Immunofluorescence localization of Cx36, LNX1 and LNX2 in brain

Immunofluorescence labelling of LNX1 in combination with labelling for Cx36 was examined in the inferior olive of mouse and rat, and in the retinal inner plexiform layer of mouse, two areas where neuronal gap junctions containing Cx36 are highly concentrated (Li *et al.*, 2004a; Kamasawa *et al.*, 2006). As previously described, immunolabelling for Cx36 appears exclusively punctate throughout the CNS, and ultrastructural studies involving freeze-fracture replica immunogold labelling (FRIL) have established its localization at neuronal gap junctions (Nagy *et al.*, 2004; Rash *et al.*, 2007a,b). Because intracellular Cx36 in neurons *in vivo* remains undetectable with currently available anti-Cx36 antibodies for reasons as yet undetermined (Nagy *et al.*, 2013; Bautista & Nagy, 2014; Rubio & Nagy, 2015), immunofluorescence localization of this connexin is considered to reveal sites *in vivo* at which it is contained in gap junctions (Nagy *et al.*, 2017, 2018). The typical punctate appearance of Cx36 labelling at neuronal gap junctions is shown in the mouse inferior olive in Figure 1A1, where we refer to this labelling as Cx36-puncta. Immunofluorescence labelling of LNX1 was also largely punctate in this structure, hence referred to as LNX1-puncta, and had a distribution very similar to that of Cx36 (Fig. 1A2). Double immunofluorescence labelling of Cx36 in combination with labelling of LNX1 showed that in overlay images many Cx36-puncta were co-localized with LNX1-puncta (Fig. 1A3), indicating localization of LNX1 to neuronal gap junctions. Conversely, not all LNX1-puncta were associated with labelling for Cx36. Where co-localization occurred, labelling for LNX1 was often confined entirely within an area occupied by individual Cx36-puncta, and sometimes LNX1 was curiously confined to small subregions of those puncta.

A control for specificity of LNX1 detection and LNX1/Cx36 co-localization was provided by the use of two LNX1 antibodies directed against different, non-overlapping sequences within this protein. Labelling patterns obtained in the inferior olive of mouse with anti-LNX1 ab247 (Fig. 1B) was similar to that obtained with anti-LNX1 ab200 (Fig. 1C), and both gave similar co-localization with Cx36 (Fig. 1B and 1C). Examination of labelling in genetically ablated LNX1 deficient mice (LNX1 KO mice) was used as a further control for localization of LNX1 at Cx36-containing gap junctions. In the inferior olive of these KO mice, labelling with both anti-LNX1 ab247 and ab200 was totally absent at Cx36-puncta (Fig. 1D and 1E). However, both antibodies produced residual punctate labelling, which appear to represent cross reaction with another as yet unidentified protein, perhaps a closely related member of the family of LNX proteins (Katoh & Katoh, 2004). Counts of

immunopositive puncta in 10-14 fields double-labelled for Cx36 and LNX1 revealed that $50 \pm 3.2\%$ and $42 \pm 3.2\%$ (mean \pm s.e.m. of the number of field examined) of Cx36-puncta were co-localized with LNX1-puncta labelled with anti-LNX1 ab200 and ab247, respectively, in sections of inferior olive from wild-type mice, while this was reduced to $2 \pm 1.2\%$ and $1 \pm 0.4\%$ Cx36-puncta co-localization with LNX1-puncta using these antibodies for labelling in sections from LNX1 KO mice. Immunofluorescence labelling of Cx36 in combination with immunolabelling of LNX1 in the inner plexiform layer of mouse retina (Fig. 2A) and in the inferior olive of rat (Fig. 2B) gave similar results as in the inferior olive of mouse. In both of these CNS regions, many Cx36-puncta displayed co-localization with LNX1 and, conversely, some LNX1-puncta in both areas showed an absence of association with Cx36-puncta.

We next examined double immunofluorescence labelling for Cx36 in conjunction with labelling for LNX2 in the inferior olive of mouse. Throughout this structure, where Cx36-puncta are abundantly found (Fig. 3A1), labelling of LNX2 had a closely matching distribution, and was also evident exclusively as immunoreactive puncta (Fig. 3A2), but the density of LNX2-puncta was somewhat less than that of Cx36-puncta (Fig. 3A3). Consistent with this observation and in contrast to results concerning LNX1, it appeared that the vast majority of LNX2-puncta were co-localized with Cx36 but, conversely, not all Cx36-puncta were associated with labelling for LNX2 (Fig. 3B and 3C). The degree of co-localization of Cx36 with LNX2 at individual puncta exhibited a variety of patterns. Where co-localization occurred, labelling for LNX2 either entirely encompassed Cx36-puncta and extended beyond the area occupied by Cx36-puncta, or was confined entirely within Cx36-puncta, occupying large to very small spatial subregions of the area circumscribed by Cx36-puncta (Fig. 3B, and C). Also frequently observed was partial overlap of labelling for Cx36 and LNX2 at individual puncta (Fig. 3B,C).

Immunoblotting and Cx36 co-IP with LNX1

Recognition of LNX1 with the rabbit polyclonal anti-LNX1 ab200 antibody we generated was demonstrated by immunoblotting of HeLa cell lysates derived from transiently transfected cells expressing LNX1p70 or LNX1p80-FLAG. In these lysates, bands were detected migrating at ~ 70 kDa and ~ 80 kDa (Fig. 4A, lanes 1 and 2), which corresponded to apparent molecular weights of LNX1p70 and LNX1p80-FLAG, respectively. These bands were absent in non-transfected wild-type (WT) cells (HeLa-WT; Fig. 4A, lane 3). Probing the same lysates with anti-FLAG revealed detection of the LNX1p80-FLAG, corresponding to this LNX1 isoform recognized by anti-LNX1, but not the non-FLAG tagged LNX1p70

isoform (Fig. 4A, lanes 4 and 5, respectively). Comparison of results with anti-LNX1 ab200 vs. ab247 after immunoblotting of these same lysates is shown in Fig. 4B, which indicated that each of these antibodies have the capacity to detect both the full-length isoform LNX1p80 and the shorter isoform LNX1p70. Immunoblotting of LNX1 and LNX2 in homogenates of brain is not shown due to difficulties in detection of these LNX isoforms in brain extracts, as also reported by others (Lenihan *et al.*, 2017b).

The molecular association of LNX1 with Cx36 was initially examined by co-IP procedures. Homogenates of mouse brain taken for IP with anti-LNX1 showed detection of Cx36 in IP material probed with anti-Cx36 (Fig. 4C, lane 3). The migration profile of the band detected in the IP material corresponded to that of Cx36 in lysates of HeLa cells stably expressing Cx36 (HeLa-Cx36) (Fig. 4C, lane 2), and this band was absent after IP with omission of anti-LNX1 (Fig. 4C, lane 4). Specificity of the band identified as Cx36 is indicated by lack of its detection in a control lane loaded with lysate from non-transfected HeLa-WT cells (Fig. 4, lane 1). In an initial pull-down experiment, we examined the interaction of Cx36 with bacterially expressed LNX1-GST fusion protein. Immunoblots of lysates of HeLa-Cx36 cells taken for pull-down with LNX1-GST and probed with anti-Cx36 showed detection of a band (Fig. 4D, lane 2) that co-migrated with Cx36 seen in input lysate from HeLa-Cx36 cells (Fig. 4D, lane 1). Further effort to examine interaction of LNX proteins with Cx36 was focused not using brain tissue, but rather transfection of cells in culture.

Immunoblotting of tissues from LNX1 null mice

To confirm that LNX1 gene targeted mice were deficient for LNX1, tissue homogenates from these mice and their wild-type counterparts were taken for immunoblotting and immunoprecipitation using LNX1 antibodies raised against distinct regions of LNX1. As expected, anti-LNX1 ab8 antibody detected LNX1p80 in wild-type tissues, but not in tissues from LNX1 KO mice (Fig. 5A). Lack of detection of LNX1p80 in lanes loaded with homogenate from wild-type small intestine is likely attributable to an insufficient amount of protein loading as indicated by only a small fraction of actin detected in lanes loaded with this tissue as compared to lanes loaded with other samples. Nonetheless, results for kidney, liver, cecum and colon provided evidence that LNX1 p80 protein was present in wild-type tissues and absent in these tissues of LNX1 KO mice. In blots of material obtained after IP with anti-LNX1 ab365 and probed with anti-LNX1 ab8 (Fig. 5B), the brain-specific LNX1p70 isoform was detected in IP material from wild-type brain, while the p80 isoform

was not detected (Fig. 5B, lane 1). In contrast, IP material from peripheral tissue homogenates (heart, colon and kidney) showed the presence of the p80 isoform and absence of the p70 isoform (Fig. 5B, lanes 3, 5, 7). After IP from tissues of LNX1 KO mice, there was an absence of LNX1 detection (Fig. 5B, lanes 2, 4, 6, 8), confirming ablation of the LNX1 in these mice and providing confidence in the identity of LNX1 bands seen in blots of IP material from wild-type tissues. Positive control IPs showed detection of LNX1p70 (Fig. 5B, lane 9) and LNX1p80 (Fig. 5B, lane 10) in IP material from lysates of LNX1p70- or LNX1p80-transfected HEK293T cells, respectively. A band migrating slightly faster than the LNX1p70 isoform seen only in IP material from wild-type brain, and which like the p70 isoform was absent after IP from brain of LNX1 KO mice, may represent the p62 isoform of LNX1 that was reported to be uniquely expressed in brain (Lenihan *et al.*, 2014). Intense bands running at an even lower molecular weight that were detected in wild-type colon and kidney (Fig. 5, lanes 5 and 7, respectively) and that were absent in LNX1 KO mice may represent degradation products of LNX1.

Pull-down of Cx36 with PDZ domains of LNX1 and LNX2

To more comprehensively examine molecular interactions between LNX proteins and Cx36 *in vitro*, bacterial fusion proteins expressed from recombinant plasmids containing His-tagged PDZ domains of LNX1 and LNX2 were used for pull-down assays. Pull-downs involved incubation of the His-PDZ domains with lysates of HeLa or N2A cells that had been transfected with either full-length Cx36 or truncated Cx36 (trCx36) lacking the C-terminal four amino acids that constitute its PDZ ligand. Immunoblots loaded with positive control input lysates and probed with anti-Cx36 showed detection of Cx36 and trCx36 in material used for pull-downs with LNX1 PDZ domains (Fig. 6A, lane 1; and 6C, lanes 2,3) or for pull-downs with LNX2 PDZ domains (Fig. 7, lanes 1,5). The Cx36 band was absent in HeLa-WT cells (Fig. 6A, lane 2 and 6C, lane 1) as well as in N2A-WT cells (not shown). Full-length Cx36 was detected after pull-down with the second PDZ domain of both LNX1 (Fig. 6A, lane 4) and LNX2 (Fig. 7A, lane 3), but was absent in pull-downs using the PDZ1, PDZ3 and PDZ4 domains of LNX1 (Fig. 6A, lanes 3, 5 and 6, respectively) or the PDZ1 and PDZ4 domains of LNX2 (Fig. 7A, lanes 2 and 4, respectively). This molecular interaction between Cx36 and the PDZ2 domains of the two LNX proteins was abrogated when pull-downs were conducted with trCx36 and either the PDZ2 domain of LNX1 (Fig. 6C, lane 5) or the PDZ2 domain of LNX2 (Fig. 7A, lane 6), indicating requirement of the Cx36 PDZ ligand for interaction of Cx36 with LNX1 or LNX2. Blots probed for pull-down material were stripped

and re-probed with monoclonal anti-His (Fig. 6B, lanes 7-12; Fig. 6D, lanes 6 and 7, which corresponded to lanes 4 and 5 in Fig. 6C; and Fig. 7B, lanes 7-12). These blots probed with anti-His showed approximately equivalent amounts of His-PDZ domain fusion proteins were used in the pull-down assays.

Localization of Cx36-eCFP, LNX1 and LNX2 in co-transfected cells

To examine the effect of LNX expression on Cx36 localization in cultured cells, N2A cells were co-transfected with Cx36-eCFP (Fig. 8) and with either LNX1p80-FLAG, LNX1p70 that lacks E3 ligase activity, LNX2-FLAG or with the functional mutant form of LNX2 (LNX2^{C51A}-FLAG) that has a mutated zinc coordination RING domain essential for ligase activity. When transfected alone into cells, the intrinsic fluorescence of Cx36-eCFP was typically distributed at both intercellular gap junctions and to punctate intracellular structures (Fig. 8A). Cells transfected with Cx36-eCFP (Fig. 8B1) and immunolabelled with anti-Cx36 (Fig. 8B2), showed co-localization of eCFP fluorescence and Cx36 immunofluorescence (Fig. 8B3), providing confidence in specificity of Cx36 detection in cultured cells. Cells co-transfected with Cx36-eCFP and LNX1p70 (Fig. 8C1) and simultaneously probed with anti-Cx36 (Fig. 8C2) and anti-LNX1 (Fig. 8C3) displayed co-localization of eCFP fluorescence, immunolabelling of Cx36 and immunolabelling of LNX1p70 at large gap junctions located at intercellular contacts and at intracellular punctate structures (Fig. 8C4). In contrast, cells co-transfected with Cx36-eCFP (Fig. 8D1) and LNX1p80-FLAG (Fig. 8D3), and probed with anti-Cx36 (Fig. 8D2) showed a loss of signals for eCFP and Cx36 at cell-cell contacts, with retention of only a fractional amount of intracellular Cx36-eCFP fluorescence. Cells expressing LNX1p80-FLAG (Fig. 8E) taken for double-labelling with anti-FLAG (Fig. 8E1) and anti-LNX1 (Fig. 8E2) showed a similar distribution of intracellular immunofluorescence for the FLAG tag and LNX1, indicating fidelity for LNX1p80-FLAG detection and confirming the diffuse nature of LNX1p80 immunoreactivity in these cells.

In cells expressing Cx36-eCFP (Fig. 8F1) and LNX2-FLAG (Fig. 8F2), and probed with anti-FLAG, there was an absence of Cx36-eCFP at cell-cell contacts suggesting lack of gap junctions, while intracellular Cx36-eCFP was retained, but at diminished levels. To determine if absence of Cx36-eCFP-containing gap junctions was dependent on the E3 ligase activity of LNX2, N2A cells were co-transfected with Cx36-eCFP and with mutant LNX2^{C51A}-FLAG. In these cells, Cx36-eCFP fluorescence was maintained at cell-cell contacts presumably reflecting gap junctions, and appeared at intense levels intracellularly (Fig. 8G1), and FLAG immunoreactivity for LNX2^{C51A}-FLAG was seen co-localized with eCFP (Fig. 8G2).

LNK2 mediated ubiquitination of Cx36

To determine if Cx36 is targeted for ubiquitination by LNK2 and if so whether ubiquitination of Cx36-eCFP by LNK2 required a functional RING domain of LNK2, lysates of cells expressing Cx36-eCFP and HA-ubiquitin together with either LNK2-FLAG, LNK2^{C51A}-FLAG or FLAG vector were taken for IP of Cx36-eCFP, immunoblotted and probed with anti-HA for detection of HA-ubiquitin conjugated to Cx36-eCFP in the IP material (Fig. 9).

The results indicated increased HA-ubiquitinated material present in IP material gathered from cells expressing LNK2-FLAG (Fig. 9A, lane 2) *vs.* those expressing the empty FLAG-vector (Fig. 9A, lane 1), and the increase was not seen in Cx36-eCFP IP material from cells expressing the LNK2^{C51A}-FLAG mutant that lacks a functional RING domain (Fig. 9A, lane 3). These results suggest that Cx36-eCFP is subject to ubiquitination mediated by LNK2, which is consistent with findings by others in studies of various targets of LNK E3 ligases, including claudins, KIF7 (kinesin-like protein), ERC2 (ERC protein2) and SRGAP2 (SLIT-ROBO Rho GTPase-activating protein 2), where ubiquitination by LNK was shown to require a functional RING domain (Lenihan *et al.*, 2014; Takahashi *et al.*, 2009). The lack of HA detection in control IPs conducted with normal rabbit IgG and lysates of the same LNK2-FLAG transfected cells used in lane 2 (Fig. 9A, lane 4) indicated that HA detection in IPs performed with anti-eGFP antibody was not due to non-specific binding of HA-ubiquitinated proteins to Protein G conjugated magnetic beads or to IgG. This latter observation suggests that our detection of baseline levels of HA-ubiquitinated Cx36-eCFP in IPs of FLAG-vector co-transfected cells was potentially due to either a small degree of non-specific IP of proteins with anti-eGFP or to the activity of an as yet unidentified endogenous E3 ubiquitin ligase on Cx36-eCFP in N2A cells. This latter possibility is consistent with observations concerning other proteins that are acted upon by multiple E3 ubiquitin ligases, including p53 and Cx43 (Chen *et al.*, 2012; Fykerud *et al.*, 2012; Satija *et al.*, 2013; Basheer *et al.*, 2015). However, we cannot at present exclude the possibility that LNK2 interacts with and mediates the ubiquitination of additional proteins that directly or indirectly associate with Cx36 and are localized at neuronal gap junctions.

Rescue of Cx36 from degradation by LNK2

We next determined if lysosomal inhibition with chloroquine or ammonium chloride could rescue the loss of Cx36-eCFP in cells overexpressing LNK2. This was examined by immunoblotting of lysates from cells co-transfected with Cx36-eCFP (Fig. 10A, lanes 1 to 7) and either LNK2-FLAG, LNK2^{C51A}-FLAG or empty FLAG vector, followed by probing of

immunoblots with anti-Cx36 ab51-6300. In cells transfected with Cx36-eCFP and co-transfected with FLAG-vector, anti-Cx36 recognized a band migrating ~60 kDa, close to the calculated molecular weight of Cx36-eCFP (Fig. 10A, lane 1), which was absent in cells transfected with FLAG-vector only (Fig. 10A, lane 8). The Cx36-eCFP band was only weakly detected in cells expressing LNX2-FLAG (Fig. 10A, lane 2), whereas the robust expression of Cx36-eCFP was retained in cells expressing the LNX2^{C51A} mutant (Fig. 10A, lane 3). When cells expressing Cx36-eCFP and LNX2 were treated with chloroquine (Fig. 10A, lanes 4-6; 10, 50, 100 mM, respectively) or 25 mM ammonium chloride (Fig. 10A, lane 7), the intense band for Cx36-eCFP was recovered. After stripping, the immunoblot shown in Figure 10A was reprobed with anti-FLAG, which showed roughly equal abundance of LNX2-FLAG in all lanes loaded with lysates from cells co-transfected with Cx36-eCFP and LNX2-FLAG (Fig. 10B, lanes 10, 12-15), as well as in lysate from cells co-transfected with Cx36-eCFP and LNX2^{C51A}-FLAG (Fig. 10B, lane 11), and its absence in cells transfected with Cx36-eCFP and FLAG-vector (Fig. 10B, lane 9), or FLAG-vector only (Fig. 10B, lane 16). These results indicate that the ultimate fate of Cx36-eCFP in cells overexpressing LNX2-FLAG was its targeting to the lysosomal compartment for degradation.

Discussion

Localization of LNX1 and LNX2 in vivo

The present results add Cx36 to the list of proteins that interact with LNX1 and/or LNX2 (LNX1/2) and that may serve as targets for ubiquitination by one or the other of these E3 ubiquitin ligases. The cellular distribution and subcellular localization of LNX1/2 proteins in the CNS has not as yet been subject to comprehensive documentation, owing perhaps to their apparently low levels of expression in neural tissue (Lenihan *et al.*, 2014), and difficulties in their detection with currently available anti-LNX antibodies. LNX1 and LNX2 mRNAs have, however, been localized by *in situ* hybridization primarily in neurons in brain (Rice *et al.*, 2001; Lenihan *et al.*, 2014), and the present immunofluorescence results indicate that at least some of those neurons correspond to neuronal populations that express Cx36. The localization of LNX1/2 specifically at sites of Cx36-puncta in the brain regions examined indicates with reasonable certainty that these E3 ligases in part reside at Cx36-containing gap junctions that form electrical synapses, because (as noted earlier) immunofluorescence labelling of Cx36 with the antibodies and immunolabelling protocols used here appears to be restricted exclusively to cellular sites at which this connexin forms gap junctions (Rash *et al.*, 2001; Nagy *et al.*, 2004; Rash *et al.*, 2007a,b; Nagy *et al.*, 2017, 2018). Although anti-LNX1

detects both p70 and p80 as shown here in transfected cells, it likely recognized LNX1p70 at these junctions given the absence of LNX1p80 expression in brain (Rice *et al.*, 2001; Lenihan *et al.*, 2014). We examined LNX1/2 association with Cx36 in only a few limited brain regions that harbor the highest density of Cx36-containing gap junctions, namely the retina and inferior olivary nucleus. However, these junctions are known to be widely distributed in brain and spinal cord (Condorelli *et al.*, 2000; Bautista *et al.*, 2014; Nagy *et al.*, 2018). Thus, it remains to be determined whether LNX1/2 proteins are similarly associated with Cx36 in other regions of the CNS.

We have previously reported the immunofluorescence localization of several other proteins at Cx36-containing gap junctions in adult rat and mouse brain, including ZO-1, AF6 (aka, afadin), cingulin and MUPP1 (Li *et al.*, 2004a, 2012; Lynn *et al.*, 2012). Labelling for some of these proteins (*e.g.*, ZO-1, cingulin) often showed total overlap of labelling with Cx36 at individual Cx36-puncta. Here, a remarkable heterogeneity was seen in the degree of overlap between labelling for LNX proteins and Cx36 at Cx36-puncta. In cases where labelling for LNX1/2 extended beyond the bounds of Cx36-puncta, LNX1/2 outside of, but contiguous with, these puncta could be associated with plasma membrane structures immediately adjacent to Cx36-puncta (*i.e.*, adherens junctions, Nagy & Lynn, 2018). Indeed, protein components of other types of cell-cell junctions, including E-cadherin at adherens junctions and claudin-1 plus occludin at tight junctions, are targets for ubiquitination by RING- and Hect-type E3 ubiquitin ligases (Fujita *et al.*, 2002; Traweger *et al.*, 2002; Takahashi *et al.*, 2009), raising the possibility that one or more of the many components of adherens junctions that flank Cx36-containing gap junctions may represent binding partners of LNX1/2. Labelling of LNX1/2 entirely confined within and occupying variable tiny to large portions of Cx36-puncta suggest that actions of LNX1/2 may be operative within subdomains of Cx36-containing gap junctions. If LNX1/2 contributes to processes governing turnover of Cx36, then these subdomains may correspond to sites within Cx36-containing gap junction plaques where a portion of this connexin may undergo removal by internalization, as has been reported to occur at gap junctions composed of other connexins (Lauf *et al.*, 2002; Gaietta *et al.*, 2002; Laird, 2006; Flores *et al.*, 2012). It is noteworthy in this context that ultrastructural studies have demonstrated endocytic annular profiles to be associated also with subdomains of Cx36-containing gap junctions between neurons in mammalian brain, specifically parvalbumin expressing neurons in the striatum, and these profiles were interpreted to represent portions of gap junctions undergoing internalization (Fukuda, 2009), which interestingly may correspond to subdomains of Cx36-puncta found to harbour

LNX1/2. In view of these considerations, it may be of interest to explore the characteristics of Cx36 turnover, morphological features and deployment of Cx36-containing gap junctions in the CNS of LNX1/2 KO mice.

Connexin E3 ubiquitin ligase interactions

Studies on the turnover, recycling and degradation of gap junctions have focused mainly on Cx43, which undergoes processing by both the lysosomal and proteasomal pathways (Leithe, 2016), with Cx43 degradation regulated by both its phosphorylation and by ubiquitination via the E3 ubiquitin ligase Nedd4, which co-localized with Cx43 at gap junctions (Leykauf *et al.*, 2006; Leithe & Rivedal, 2004; Leithe *et al.*, 2006; Leithe & Rivedal, 2007). These findings suggested that Cx43 was ubiquitinated at gap junctions within the plasma membrane, which signalled Cx43 for ultimate proteasomal degradation. Subsequently, Cx43 was found to undergo ubiquitination by other E3 ubiquitin ligases (Chen *et al.*, 2012; Fykerud *et al.*, 2012; Basheer *et al.*, 2015), and additional connexins were reported to be ubiquitinated, including connexin26, connexin32 and connexin40 (Leithe, 2016). We now add Cx36 to this list, which expands the growing number of substrates and/or binding partners of LNX1/2 proteins that were identified by biochemical or proteomic methods and by strategies that combined biochemical approaches with bioinformatic analysis (Song *et al.*, 2006; Wolting *et al.*, 2011; Guo *et al.*, 2012).

Our finding that the classical C-terminal four amino acid PDZ ligand of Cx36 (*i.e.*, SAYV), which is required for interaction of Cx36 with PDZ domains in AF6, MUPP1 and of ZO-1 (Li *et al.*, 2004a, 2009, 2012), mediates Cx36 association with the PDZ2 domains of both LNX1 and LNX2 is consistent with the highly homologous sequence of these two LNX proteins, particularly in regions that define their substrate specificity (Rice *et al.*, 2001; Flynn *et al.*, 2011). Based on our results from transfected cells in culture, it is likely that association of LNX1/2 with electrical synapses in brain arises by virtue of Cx36 PDZ ligand interaction with the PDZ2 domains in LNX1/2. This was supported by co-localization of Cx36-containing gap junctions with both the catalytically inactive LNX1p70 isoform and LNX2 isoform bearing an E3-ubiquitin ligase loss of function mutation in transfected cells. These results suggested LNX1/2 targeting to Cx36 at the plasma membrane, similar to such targeting of the E3 ubiquitin ligase Nedd4 to gap junctions composed of Cx43 ((Leithe, 2016). Co-localization of Cx36 with LNX1p80 or LNX2 in transfected cells was not observed due to the loss of Cx36 at cell-cell contacts, which was interpreted to indicate a potential ubiquitin-related mechanism for degradation of Cx36 by these E3 ligase-competent

isoforms of LNX1/2, as supported by the observed retention of Cx36-containing gap junctions in cells expressing the LNX2 loss of function mutant. Consistent with this idea was that ubiquitination of Cx36-eCFP in the presence of LNX2 was not observed in cells transfected with the LNX2^{CS1A} mutant. Further, the observed loss of Cx36-eCFP in cells expressing LNX2 was not seen in cells expressing mutant LNX2 lacking a functional RING domain. In addition, the loss of Cx36-eCFP detection seen in the presence of LNX2 was abrogated by treatment of LNX2-expressing cells with inhibitors of lysosomal degradation, suggesting that one mechanism for ubiquitinated Cx36 degradation is via the lysosomal pathway, similar to processing of Cx43 after its Nedd1-mediated ubiquitination or to the ubiquitination and degradation of claudins in MDCK cells overexpressing LNX1, and recovery of claudin detection in these cells by treatment with lysosome inhibitors (Leithe, 2016; Takahashi *et al.*, 2009).

Results concerning LNX1p80, although consistent with those involving LNX2, are perhaps less physiologically relevant given the absence of LNX1p80 expression in adult brain as seen here and reported by others (Rice *et al.*, 2001; Lenihan *et al.*, 2014). In this regard, it is noteworthy that both LNX1 and LNX2 contain, in addition to four unique PDZ domains, classical C-terminal PDZ ligand motifs, and LNX1 was shown to interact with LNX2 and has a similar cell-type expression pattern and regional distribution as LNX2 (Rice *et al.*, 2001; Lenihan *et al.*, 2014). It has been suggested that the observed self-binding of the PDZ1 domains of LNX1/2 with their own C-terminal PDZ ligands may serve to inhibit interaction with target PDZ ligands, providing a mechanism for self-regulating their actions on target proteins (Rice *et al.*, 2001). Our results showing the presence of both LNX1/2 at Cx36-containing neuronal gap junctions, together with our findings and reports that only LNX1 protein isoforms that lack E3 ligase activity are expressed in brain (Rice *et al.*, 2001; Lenihan *et al.*, 2014), suggest that LNX1 at electrical synapses may confer stability on these synapses via PDZ-mediated regulatory interactions with LNX2 that inhibit the E3 ligase activity of LNX2 on Cx36. Alternatively, the association of E3 ligase-incompetant LNX1p70 with Cx36 may moderate, in a competitive manner, the availability of Cx36 for interaction with ligase-competant LNX2.

Sequence analyses have revealed that the LNX1/2 genes are ancestrally related to the multi-PDZ domain protein1 (MUPP1) that contains thirteen PDZ domains, the last four (PDZ 10-13) of which share similar splice junctions and primary sequence homology with PDZ1-4 domains of LNX1/2 (Flynn *et al.*, 2011). Computed potential PDZ interactions (Hui *et al.*, 2010) revealed that almost all proteins predicted to interact with the PDZ1 or PDZ2 domains

of LNX1/2 do interact with either PDZ10 or PDZ11 of MUPP1 (Flynn *et al.*, 2011). It was shown empirically that interactors with MUPP1 PDZ10-13, including the synaptic proteins SynGap1 (synaptic GTPase activating protein) and HTR2C (Serotonin receptor 2C subunit), also interacted with the PDZ1 and 2 domains of LNX1/2 (Flynn *et al.*, 2011). These predictive/empirical findings are supported by our previous report on the interaction of Cx36 with the 10th PDZ domain of MUPP1 (Li *et al.*, 2012) taken together with the present demonstration of Cx36 interaction with the PDZ2 domains of LNX1/2.

Conclusions

Mechanisms underlying the dynamic nature and reported plasticity of electrical synapses formed by Cx36-containing neuronal gap junctions may be diverse, and the biochemical correlates of these mechanisms may be commensurate with an equally diverse composition of structural and regulatory proteins associated with these synapses. Thus, in addition to various previously reported cellular processes that could potentially influence the efficacy of electrical synaptic transmission (Pereda *et al.*, 2013; Pereda, 2014; Nagy *et al.*, 2018), the actions of LNX1/2 at electrical synapses composed of Cx36 could in part provide the basis for the steady-state turnover of Cx36 at gap junctions. These LNX isoforms may also govern rapid, moment-to-moment trafficking of Cx36-containing channels at these junctions, thereby regulating the availability of functional channels for mediation of electrical coupling.

Acknowledgements

This work was supported by grants from the Canadian Institutes of Health Research and the Canadian Natural Sciences and Engineering Research Council to J.I. Nagy and to C.J. McGlade. We thank Dr. R. Hall for bacterial expression plasmids containing the His-tagged PDZ domains of LNX1 and LNX2, and B. McLean for excellent technical assistance.

Author contributions

B.D.L. conducted the molecular, IP, pull-down and immunofluorescence studies involving cell cultures; X.L. conducted IP and pull-down of Cx36 with LNX1 using brain tissues, J.I.N. was responsible for the immunofluorescence work involving brain sections; S.G.H. contributed the Cx36-eCFP for transfection approaches and design of the work involving this construct; C.J.M. and E.K.G. generated the LNX1 C57BL/6 null mice, LNX1 and LNX2 expression constructs, the full length LNX1-GST fusion protein construct and LNX1 antibodies used for immunoprecipitation; and B.D.L., X.L. and J.I.N. participated in data analysis, figure compilation and wrote the manuscript, with final critical evaluation of data interpretation, intellectual content and manuscript approval provided by C.J.M. and S.G.H.

Competing financial interests

The authors declare no competing financial interests.

Data statement

The raw data will not be deposited in a public repository due to the complexity of its assembly, but it can be obtained upon request to the corresponding author.

Abbreviations

co-IP, co-immunoprecipitation; CNS, central nervous system; Cx36, connexin36; eCFP, enhanced cyan fluorescent protein; eGFP, enhanced green fluorescent protein; IP, immunoprecipitation; LNX1, ligand of NUMB protein X1; LNX2, ligand of NUMB protein X2; LNX1/2, LNX1 and LNX2; MUPP1, multi-PDZ domain protein1; PBS, 50 mM sodium phosphate buffer, pH 7.4, containing 0.9% NaCl; PDZ, PSD-95/SAP90, DlgA, ZO-1; PVDF, polyvinylidene difluoride; RIPA buffer, 50 mM Tris pH 8.0, 150 mM NaCl, 1.0% IGEPAL CA-630, 0.5% sodium deoxycholate; SDS-PAGE, sodium dodecylsulphate polyacrylamide gel electrophoresis; TBS, 50 mM Tris-HCl, pH 7.4, containing 1.5% sodium chloride; TBSTr, TBS containing 0.3% Triton X-100; TBS-Tw, 20 mM Tris pH 7.4, 150 mM NaCl, 0.2% Tween-20 and 5% skim milk powder; trCx36, truncated Cx36; ZO, zonula occludens.

References

- Basheer, W.A., Harris, B.S., Mentrup, H.L., Abreha, M., Thames, E.L., Lea, J.B., Swing, D.A., Copeland, N.G., Jenkins, N.A., Price, R.L. & Matesic, L.E. (2015) Cardiomyocyte-specific overexpression of the ubiquitin ligase Wwp1 contributes to reduction in Connexin43 and arrhythmogenesis. *J. Mol. Cell Cardiol.*, **88**, 1-13.
- Bautista, W., McCrea, D.A. & Nagy, J.I. (2014) Connexin36 identified at morphologically mixed chemical/electrical synapses on trigeminal motoneurons and at primary afferent terminals on spinal cord neurons in adult mouse and rat. *Neuroscience*, **263**, 159-180.
- Bautista, W. & Nagy, J.I. (2014) Connexin36 in gap junctions forming electrical synapses between motoneurons in sexually dimorphic motor nuclei in spinal cord of rat and mouse. *Eur. J. Neurosci.*, **39**, 771-787.
- Bennett, M.V.L. (1997) Gap junctions as electrical synapses. *J. Neurocytol.*, **26**, 349-366.
- Bennett, M.V.L. & Zukin, S.R. (2004) Electrical coupling and neuronal synchronization in the mammalian brain. *Neuron*, **41**, 495-511.
- Berthoud, V.M., Minoque, P.J., Laing, J.G. & Beyer, E.C. (2004) Pathways for degradation of connexins and gap junctions. *Cardiovas. Res.*, **62**, 256-267.
- Bhoj, V.G. & Chen, Z.J. (2009) Ubiquitylation in innate and adaptive immunity. *Nature*, **458**, 430-437.
- Bloomfield, S.A. & Volgyi, B. (2009) The diverse functional roles and regulation of neuronal gap junctions in the retina. *Nature Rev. Neurosci.*, **10**, 495-506.
- Chen, V.C., Kristensen, A.R., Foster, L.J. & Naus, C.C. (2012) Association of connexin43 with E3 ubiquitin ligase TRIM21 reveals a mechanism for gap junction phosphodegron control. *J. Proteome Res.*, **11**, 6134-6146.
- Condorelli, D.F., Belluardo, N., Trovato-Salinaro, A. & Mudo, G. (2000) Expression of Cx36 in mammalian neurons. *Brain Res. Rev.*, **32**, 72-85.

Connors, B.W. (2009) Electrical signaling with neuronal gap junctions. In: A.Harris, D.Locke (Eds.), *Connexins: A Guide*, Humana Press/Springer, pp. 143-164.

Curti, S. & O'Brien, J. (2016) Characteristics and plasticity of electrical synaptic transmission. *BMC Cell Biol.*, **17**, 59-70.

Dai, M.S. & Lu, H. (2004) Inhibition of MDM2-mediated p53 ubiquitination and degradation by ribosomal protein L5. *J. Biol. Chem.*, **279**, 44475-44482.

Deshaies, R.J. & Joazeiro, C.A.P. (2009) Ring domain E3 ubiquitin ligases. *Annu. Rev. Biochem.*, **78**, 399-434.

D'Agostino, M., Tornillo, G., Caporaso, M.G., Barone, M.V., Ghigo, E., Bonatti, S. & Mottola, G. (2011) Ligand of Numb proteins LNX1p80 and LNX2 interact with the human glycoprotein CD8 α and promote its ubiquitylation and endocytosis. *J. Cell Sci.*, **124**, 3545-3556.

Dho, S.E., Jacob, S., Wolting, C.D., French, M.B., Rohrschneider, L.R. & McGlade, C.J. (1998) The mammalian numb phosphotyrosine-binding domain. Characterization of binding specificity and identification of a novel PDZ domain-containing numb binding protein, LNX. *J. Biol. Chem.*, **273**, 9179-9187.

Evans, W.H. & Martin, P.E.M. (2002) Gap junctions: structure and function. *Mol. Membr. Biol.*, **19**, 121-136.

Fam, S.R., Paquet, M., Castleberry, A.M., Oller, H., Lee, C.J., Traynelis, S.F., Smith, Y., Yun, C.C. & Hall, R.A. (2005) P2Y1 receptor signaling is controlled by interaction with the PDZ scaffold NHERF-2. *Proc. Natl. Acad. Sci.*, **102**, 8042-8047.

Flores, C.E., Nannapanenia, S., Davidson, K.G.V., Thomas Yasumura, T., Bennett, M.V.L., Rash, J.E. & Pereda, A.E. (2012) Trafficking of gap junction channels at a vertebrate electrical synapse in vivo. *Proc. Natl. Acad. Sci.*, **109**, 573-582.

Flynn, M., Saha, O. & Young, P. (2011) Molecular evolution of the LNX gene family. *BMC Evol. Biol.*, **11**, 1-14.

Fujita, Y., Krause, G., Scheffner, M., Zechner, D., Leddy, H.E., Behrens, J., Sommer, T. & Birchmeier W. (2002) Hakai, a c-Cbl-like protein, ubiquitinates and induces endocytosis of the E-cadherin complex. *Nat. Cell Biol.*, **4**, 222-231.

Fukuda, J. (2009) Network architecture of gap junction-coupled neuronal linkage in the striatum. *J. Neurosci.*, **29**, 1235-1243.

Flykerud, T.A., Kjenseth, A., Schink, K.O., Sirnes, S., Bruun, J., Omori, Y., Brech, A., Rivedal, E. & Leithe, E. (2012) Smad ubiquitination regulatory factor-2 controls gap junction intercellular communication by modulating endocytosis and degradation of connexin43. *J. Cell Sci.*, **125**, 3966–3976.

Gaietta, G., Deerinck, T.J., Adams, S.R., Bouwer, J., Tour, O., Larid, D.W., Sosinsky, G.E., Tsien, R.Y. & Ellisman, M.H.. (2002) Multicolor and electron microscopic imaging of connexin trafficking. *Science*, **296**, 503–507.

Goodenough, D.A. & Paul D.L. (2009) Gap junctions. *Cold Spring Harb. Perspect. Biol.*, 1-19, 1:a002576.

Guo, Z., Song, E., Ma, S., Wang, X., Gao, S., Shao, C., Hu, S., Jia, L., Tian, R., Xu, T. & Gao, Y. (2012) Proteomics strategy to identify substrates of LNX, a PDZ domain-containing E3 ubiquitin ligase. *J. Proteome Res.*, **11**, 4847-4862.

Haas, J.S., Zavala, B. & Landisman, C.E. (2011) Activity-dependent long-term depression of electrical synapses. *Science*, **334**, 389-393.

Haas, J.S., Greenwald, C.M. & Pereda, A.E. (2016) Activity-dependent plasticity of electrical synapses: increasing evidence for its presence and functional roles in the mammalian brain. *BMC Cell Biol.*, **17**, 51-57.

Helbig, I., Sammler, E., Eliava, M., Bolshakov, A.P., Rozov, A., Bruzzone, R., Monyer, H. & Hormuzdi, S.G. (2010) In vivo evidence for the involvement of the carboxy terminal domain in assembling connexin36 at the electrical synapse. *Mol. Cell Neurosci.*, **45**, 47-58.

Herve, J.C., Derangeon, M., Sarrouilhe, D., Giepmans, B.N.G. & Bourmeyster, N. (2012) Gap junctional channels are parts of multiprotein complexes. *Biochim. Biophys. Acta*, **1818**, 1844-1865.

Hormuzdi, S.G., Filippov, M.A., Mitropoulou, G., Monyer, H. & Bruzzone, R. (2004) Electrical synapses: a dynamic signaling system that shapes the activity of neuronal networks. *Biochim. Biophys. Acta*, **1662**, 113-137.

Hui, S. & Bader, G.D. (2010) Proteome scanning to predict PDZ domain interactions using support vector machines. *BMC Bioinformatics*, **11**, 1-14.

Kamitani, T., Kito, K., Nguyen, H.P. & Yeh, E.T. (1997) Characterization of NEDD8, a developmentally down-regulated ubiquitin-like protein. *J. Biol. Chem.*, **272**, 28557-28562.

Kamasawa, N., Furman, C.S., Davidson, K.G.V., Sampson, J.A., Magnie, A.R., Gebhardt, B.R., Kamasawa, M., Yasumura, T., Zumbrennen, J.R., Pickard, G.E., Nagy J.I. & Rash, J.E. (2006) Abundance and ultrastructural diversity of neuronal gap junctions in the OFF and ON sublaminae of the inner plexiform layer of rat and mouse retina. *Neuroscience*, **142**, 1093-1117.

Katoh, M. & Katoh, M. (2004) Identification and characterization of PDZRN3 and PDZRN4 genes in silico. *Int. J. Mol. Med.*, **13**, 607-613.

Kjenseth, A., Fykerud, T., Rivedal, E. & Leithe, E. (2010) Regulation of gap junction intercellular communication by the ubiquitin system. *Cell Signal.*, **22**, 1267-1273.

Kothmann, W.W., Massey, S.C. & O'Brien J. (2009) Dopamine-stimulated dephosphorylation of Connexin 36 mediates AII amacrine cell uncoupling. *J. Neurosci.*, **29**, 14903-14911.

Laird, D.W. (2006) Life cycle of connexins in health and disease. *Biochem. J.*, **394**, 527–543.

Lauf, U., Giepmans, B.N., Lopez, P., Braconnot, S., Chen, S.C. & Falk, M.M. (2002) Dynamic trafficking and delivery of connexons to the plasma membrane and accretion to gap junctions in living cells. *Proc.Natl. Acad. Sci.*, **99**, 10446–10451.

Leithe, E. & Rivedal, E. (2004) Epidermal growth factor regulates ubiquitination, internalization and proteasome-dependent degradation of connexin43. *J. Cell Sci.*, **117**, 1211–1220.

Leithe, E., Brech, A. & Rivedal, E. (2006) Endocytic processing of connexin43 gap junctions: a morphological study. *Biochem. J.*, **393**, 59–67.

Leithe, E. & Rivedal, E. (2007) Ubiquitination of gap junction proteins. *J. Membr. Biol.*, **217**, 43–51.

Leithe, E. (2016) Regulation of connexins by the ubiquitin system: Implications for intercellular communication and cancer. *Biochim. Biophys. Acta*, **1865**, 133–146.

Lenihan, J.A., Saha, O., Mansfield, L.M. & Young, P.W. (2014) Tight, cell type-specific control of LNX expression in the nervous system, at the level of transcription, translation and protein stability. *Gene*, **552**, 39–50.

Lenihan, J.A., Saha, O. & Young, P.W. (2017a) Proteomic analysis reveals novel ligands and substrates for LNX1 E3 ubiquitin ligase. *PLoS One*, **12**:e0187352.

Lenihan, J.A., Saha, O., Heimer-McGinn, V., Cryan, J.F., Feng, G. & Young, P.W. (2017b) Decreased anxiety-related behaviour but apparently unperturbed NUMB function in ligand of NUMB protein-X (LNX) ½ double knockout mice. *Mol. Neurobiol.*, **54**, 8090–8109.

Leykauf, K., Salek, M., Bomke, J., Frech, M., Lehmann, W.D., Durst, M. & Alonso, A. (2006) Ubiquitin protein ligase Nedd4 binds to connexin43 by a phosphorylation-modulated process. *J. Cell Sci.*, **119**, 3634–3642.

Li, X., Olson, C., Lu, S., Kamasawa, N., Yasumura, T., Rash, J.E. & Nagy, J.I. (2004a) Neuronal connexin36 association with zonula occludens-1 protein (ZO-1) in mouse brain and interaction with the first PDZ domain of ZO-1. *Eur. J. Neurosci.*, **19**, 2132-2146.

Li, X., Olson, C., Lu, S. & Nagy, J.I. (2004b) Association of connexin36 with zonula occludens-1 in HeLa cells, β TC-3 cells, pancreas and adrenal gland. *Histochem. Cell Biol.*, **122**, 485-498.

Li, X., Lu, S. & Nagy, J.I. (2009) Direct association of connexin36 with zonula occludens-2 and zonula occludens-3. *Neurochem. Int.*, **54**, 393-402.

Li, X., Lynn, B.D. & Nagy, J.I. (2012) The effector and scaffolding proteins AF6 and MUPP1 interact with connexin36 and localize at gap junctions that form electrical synapses in rodent brain. *Eur. J. Neurosci.*, **35**, 166-181.

Lynn, B.D., Li, X. & Nagy, J.I. (2012) Under construction: Building the macromolecular superstructure and signaling components of an electrical synapse. *J. Membr. Biol.*, **245**, 303-317.

Miller, A.C. & Pereda, A.E. (2017) The electrical synapse: molecular complexities at the gap and beyond. *Develop. Neurobiol.*, **77**, 562–574.

Nagy, J.I., Dudek, F.E. & Rash, J.E. (2004) Update on connexins and gap junctions in neurons and glia in the mammalian nervous system. *Brain Res. Rev.*, **47**, 191-215.

Nagy, J.I., Bautista, W., Blakley, B. & Rash, J.E. (2013) Morphologically mixed chemical-electrical synapses formed by primary afferents in rodent vestibular nuclei as revealed by immunofluorescence detection of connexin36 and vesicular glutamate transporter-1. *Neuroscience*, **252**, 468-488.

Nagy, J.I., Pereda, A.E. & Rash, J.E. (2017) On the occurrence and enigmatic functions of mixed (chemical plus electrical) synapses in the mammalian CNS. *Neurosci. Lett.*, pii **17**, 30755-3. 10.1016/j.neulet.2017.09.021, [Epub ahead of print].

Nagy, J.I., Pereda, A.E. & Rash, J.E. (2018) Electrical synapses in mammalian CNS: Past eras, present focus and future directions. *Biochim. Biophys. Acta*, **1860**, 102-123.

Nagy, J.I. & Lynn, B.D. (2018) Structural and intermolecular associations between connexin36 and other protein components at the adherens junction-neuronal gap junction complex. *Neuroscience*, In Press.

Nie, J., McGill, M.A., Dermer, M., Dho, S.E., Wolting, C.D., McGlade, C.J. (2002) LNX functions as a RING type E3 ubiquitin ligase that targets the cell fate determinant Numb for ubiquitin-dependent degradation. *EMBO J.*, **21**, 93-102.

O'Brien, J. (2014) The ever-changing electrical synapse. *Curr. Opin. Neurobiol.*, **29**, 64-72.

Palacios-Prado, N., Hoge G., Marandykina, A., Rimkute L., Chapuis, S., Paulauskas, N., Skeberdis, W.A., O'Brien, J., Pereda, A.E., Bennett, M.V.L. & Bukauskas, F.F. (2013) Intracellular magnesium-dependent modulation of gap junction channels formed by neuronal connexin36. *J. Neurosci.*, **33**, 4741-4753.

Palacios-Prado, N., Chapuis, S., Panjkovich, A., Fregeac, J., Nagy, J.I. & Bukauskas, F.F. (2014) Molecular determinants of magnesium-dependent synaptic plasticity at electrical synapses formed by connexin36. *Nature Comm.*, **5**, 1-13. DOI: 10.1038/ncomms5667.

Pereda, A.E., Curti, S., Hoge, G., Cachope, R., Flores, C.E. & Rash, J.E. (2013) Gap junction-mediated electrical transmission: Regulatory mechanisms and plasticity. *Biochim. Biophys. Acta*, **1828**, 134-146.

Pereda, A.E. (2014) Electrical synapses and their functional interactions with chemical synapses. *Nature Rev. Neurosci.*, **15**, 250-263.

Rash, J.E., Yasumura, T., Dudek, F.E. & Nagy, J.I. (2001) Cell-specific expression of connexins and evidence of restricted gap junctional coupling between glial cells and between neurons. *J. Neurosci.*, **21**, 1983-2000.

Rash, J.E., Olson, C.O., Davidson, K.G., Yasumura, T., Kamasawa, N. & Nagy, J.I. (2007a) Identification of connexin36 in gap junctions between neurons in rodent locus coeruleus. *Neuroscience*, **147**, 938-956.

Rash, J.E., Olson, C.O., Pouliot, W.A., Davidson, K.G., Yasumura, T., Furman, C.S., Royer, S., Kamasawa, N., Nagy, J.I. & Dudek, F.E. (2007b) Connexin36 vs. connexin32, "miniature" neuronal gap junctions, and limited electrotonic coupling in rodent suprachiasmatic nucleus. *Neuroscience*, **149**, 350-371.

Rice, D.S., Northcutt, G.M. & Kurschner, C. (2001) The Lnx family proteins function as molecular scaffolds for Numb family proteins. *Mol. Cell. Neurosci.*, **18**, 525-540.

Rubio, M.E. & Nagy, J.I. (2015) Connexin36 expression in major centers of the auditory system in the CNS of mouse and rat: evidence for neurons forming purely electrical synapses and morphologically mixed synapses. *Neuroscience*, **303**, 604-629.

Satija, Y.K., Bhardwaj, A. & Das, S. (2013) A portrayal of E3 ubiquitin ligases and deubiquitylases in cancer. *Int. J. Cancer*, **133**, 2759-2768.

Song, E., Gao, S., Tian, R., Ma, S., Huang, H., Guo, J., Li, Y., Zhang, L. & Gao, Y. (2006) A high efficiency strategy for binding property characterization of peptide-binding domains. *Mol. Cell Proteomics*, **5**, 1368-1381.

Takahashi, S., Iwamoto, N., Sasaki, H., Ohashi, M., Oda, Y., Tsukita, S. & Furuse, M. (2009) The E3 ubiquitin ligase LNX1p80 promotes the removal of claudins from tight junctions in MDCK cells. *J. Cell Sci.*, **122**, 985-994.

Traweger, A., Fang, D., Liu, Y.C., Stelzhammer, W., Krizbai, I.A., Fresser, F., Bauer, H.C. & Bauer, H. (2002) The tight junction-specific protein occludin is a functional target of the E3 ubiquitin-protein ligase itch. *J. Biol. Chem.*, **277**, 10201-10208.

Urschel, S., Hoher, T., Schubert, T., Alev, C., Sohl, G., Worsdorfer, P., Asahara, T., Dermietzel, R. Weiler, R. & Willecke, K. (2006) Protein kinase A-mediated phosphorylation

of connexin36 in mouse retina results in decreased gap junctional communication between AII amacrine cells. *J. Biol. Chem.*, **281**, 33163-33171.

Wang, H.Y., Lin, Y.P., Mitchell, C.K., Ram, S. & O'Brien, J. (2015) Two-color fluorescent analysis of connexin36 turnover: relationship to functional plasticity. *J. Cell Sci.*, **128**, 3888-3897.

Wolting, C.D., Griffiths, E.K., Sarao, R., Prevost, B.C., Wybenga-Groot, L.E. & McGlade, C.J. (2011) Biochemical and computational analysis of LNX1 interacting proteins. *PLoS ONE*, **6**, e26248.

Xie, Y., Zhao, W., Wang, W., Zhao, S., Tang, R., Ying, K., Zhou, Z. & Mao, Y. (2001) Identification of a human LNX protein containing multiple PDZ domains. *Biochem. Genet.*, **39**, 117-126.

Ye, F. & Zhang, M. (2013) Structures and target recognition modes of PDZ domains: recurring themes and emerging pictures. *Biochem. J.*, **455**, 1-14.

Figure legends

Fig. 1. Immunofluorescence co-localization of LNX1 with Cx36 in the inferior olive of adult mouse. The series of three images (1-3) for each of A to E show the same field double-labelled for Cx36 (red) and LNX1 (green), with image merge where red/green overlap appears yellow. (A) Low magnification showing the punctate appearance and relative density of immunolabelling for Cx36 (A1) and LNX1 (A2), and a high degree of co-localization (A3). (B,C) Higher magnifications showing labelling of Cx36 in combination with anti-LNX1 ab247 (B) or anti-LNX1 ab200 (C). Most Cx36-puncta are co-localized with LNX1 (arrows), but not all LNX1-puncta are associated with Cx36-puncta (arrowheads). (D,E) Labelling of Cx36 with anti-LNX1 ab247 (D) or anti-LNX1 ab200 (E) in the inferior olive of LNX1 KO mice. Both anti-LNX1 antibodies produce residual punctate labelling (D,E, arrowheads), but Cx36-puncta are totally devoid of labelling for LNX1, as seen in overlays (D3,E3, arrows).

Fig. 2. Immunofluorescence co-localization of LNX1 with Cx36 in the retina of adult mouse and the inferior olive of adult rat. (A) Inner plexiform layer of mouse retina, showing Cx36-puncta (A1, arrows) and in the same field immunolabelling with anti-LNX1 ab200 (A2, arrows), with overlay showing nearly all Cx36-puncta co-localized with LNX1 (A3, arrows). (B) Rat inferior olive showing Cx36-puncta (B1, arrows) and in the same field labelling with anti-LNX1 ab247 (B2, arrows), with overlay showing all Cx36-puncta co-localized with LNX1 (B3, arrows), as also shown at higher magnification in inset. In both mouse retina and rat IO, not all labelling for LNX1 is associated with Cx36.

Fig. 3. Immunofluorescence co-localization of LNX2 with Cx36 in the inferior olive of adult mouse. (A) Low magnification showing punctate appearance of labelling for both Cx36 (A1, arrows) and LNX2 (A2, arrows), with substantial co-localization of puncta (A3, arrows). (B,C) Laser scanning confocal images of double labelling for Cx36 and LNX2 shown in overlay. At sites of Cx36 co-localization with LNX2, Cx36-puncta appear either within the confines of labelling for LNX2 (B, arrows) or display only partial overlap with LNX2-puncta (C, arrowheads). Some Cx36-puncta display only a very small portion of their area occupied by labelling for LNX2 (C, inset).

Fig 4. Immunoblots showing detection of LNX1p70 and LNX1p80 in transiently transfected HeLa cells, detection of Cx36 after IP of LNX1 from brain, and pull-down of Cx36 with GST-LNX1. (A) Blots of lysates from HeLa cells transiently transfected with LNX1p80-FLAG or LNX1-p70, as indicated, and probed with anti-LNX1 (lanes 1-3) or anti-FLAG (lanes 4, 5), showing detection of LNX1p80 isoform migrating at ~80 kDa (lane 1) and the LNX1p70 isoform migrating at ~70 kDa (lane 2), and absence of these bands in HeLa-WT cells (lane 3). Lanes probed with anti-FLAG show detection of LNX1p80-FLAG (lane 4) and lack of detection of untagged LNX1p70 (lane 5). (B) Blots of lysates from HeLa cells transiently transfected with LNX1p80-FLAG or LNX1-p70, as indicated, and probed with anti-LNX1 ab247 (lanes 1, 2) or ab200 (lanes 3, 4), showing detection of both LNX1p80 and p70 isoform with each of the antibodies. (C) Blot probed with anti-Cx36 showing detection of Cx36 (lane 3) in material immunoprecipitated from mouse brain with anti-LNX1. Controls show a corresponding Cx36 band from lysate of HeLa-Cx36 cells (lane 2) and absence of this band in lysate of HeLa-WT (lane 1) or in immunoprecipitate from brain after antibody omission (lane 4). (D) Pull-down of Cx36 from HeLa-Cx36 cells with full-length GST-tagged LNX1, showing a blot probed with anti-Cx36 and detection of a Cx36 band in pull-down material (lane 2) corresponding to a band detected in lysate from HeLa-Cx36 cells.

Fig. 5. Confirmation of LNX1 detection in tissues from wild-type mice and its absence in LNX1 KO mice. LNX1 protein expression and immunoprecipitation of LNX1 isoforms in tissues from wild type mice and absence of LNX1 protein in tissues from LNX1 gene ablated mice. (A) Total protein homogenates from adult wild-type (WT) and LNX1 knockout (KO) mouse tissues were immunoblotted with the anti-LNX1 ab8. LNX1p80 was detected in lanes loaded with proteins from wild-type kidney (lane 2), liver (lane 4), cecum (lane 8) and colon (lane 10), but not in adjacent lanes loaded with proteins of these tissues taken from LNX1 KO mice (lanes 3, 5, 9, 11), showing lack of LNX1 expression in LNX1 KO mice. A positive control lane was loaded with protein lysate from LNX1p80 transfected HEK293T cells (lane 1). The same blot was stripped and reprobed with anti-actin antibody (lower panel). LNX1 was not detected in lanes loaded with homogenate from wild-type (lane 6) or KO (lane 7) small intestine, possibly due to inadequate protein loading. (B) LNX1 IP from tissue homogenates of wild-type or LNX1 KO mice and from lysates of LNX1p70- or LNX1p80-transfected HEK293T cells using anti-LNX1 ab365 or rabbit IgG control, with immunoblots of IP material probed using anti-LNX1 ab8. Positive control IP shows migration profiles of LNX1 isoforms in IP material from the transfected HEK293T cells (lanes 9 and 10). Brain IP

material showed the presence of LNX1p70, but absence of LNX1p80 (lane 1). LNX1p80 but not LNX1p70 was detected in IP material of wild-type heart (lane 3), colon (lane 5) and kidney (lane 7), all of which as well as IP material of brain showed an absence of LNX1 protein isoforms in LNX1 KO mice (lanes 2, 4, 6, 8). No bands were detected after control IP conducted with normal rabbit IgG using wild-type brain homogenate (lane 11), LNX1p70-transfected HEK293T cell lysate (p80-nr; lane 12) or LNX1p80-transfected HEK293T cell lysate (p80-nr; lane 13).

Fig. 6. Selective interaction of Cx36 with the second PDZ domain of LNX1, and requirement of Cx36 PDZ ligand for interaction. (A) Blot probed with anti-Cx36 after pull-down of Cx36 from HeLa-Cx36 cells with PDZ domains of LNX1, showing detection of Cx36 after pull-down with PDZ2 domain (lane 4), but not after pull-down with PDZ1 (lane 3), PDZ3 (lane 5) or PDZ4 (lane 6) domains of LNX1. The Cx36 pull-down band corresponds to Cx36 detected in lysates from HeLa-Cx36 cells (lane 1), which is absent in HeLa-WT (lane 2). (B) The same blot as in (A) stripped and re-probed with anti-His (lanes 7-12) shows equivalent presence of the PDZ1-4 domains used for pull-downs (lanes 9-12), and absence of His-tag in HeLa-Cx36 and HeLa-WT cells (lanes 7 and 8). (C) Blot probed with anti-Cx36 (lanes 1-5) shows pull-down of Cx36 with the PDZ2 domain of LNX1 (lane 4) from lysates of HeLa-Cx36 cells, and lack of pull-down with PDZ2 from HeLa cells expressing Cx36 truncated of its 4 amino acid C-terminus PDZ ligand (trCx36; lane 5). Controls show detection of Cx36 (lane 2) and trCx36 (lane 3) in lysates from HeLa-Cx36 or HeLa-trCx36 cells, respectively, and absence of Cx36 in HeLa-WT cells (lane 1). (D) Lanes 4 and 5 were stripped and re-probed with anti-His to show equal loading of the PDZ2 domain used for pull-down (lanes 6 and 7).

Fig. 7. Selective interaction of Cx36 with the second PDZ domain of LNX2, and dependence on the PDZ ligand of Cx36 for interaction. (A) Blot probed with anti-Cx36 (lanes 1-6) shows detection of Cx36 in pull-down from lysate of N2A-Cx36 cells using the PDZ2 domain of LNX2 (lane 3), and absence of Cx36 pull-down from lysates of these cells using the PDZ1 and PDZ4 domains of LNX2. Also absent is PDZ2 domain pull-down of Cx36 from N2A cells expressing Cx36 devoid of its PDZ ligand (trCx36) (lane 6). Controls show detection of Cx36 (lane 1) and trCx36 (lane 5) in transiently transfected N2A cells. A dimer form of Cx36 was also detected (lanes 1, 3, and 5). (B) The same blot stripped and re-probed with anti-His (lanes 7-12) shows equivalent amounts of PDZ1, PDZ2 and PDZ4 domains of LNX2 used for

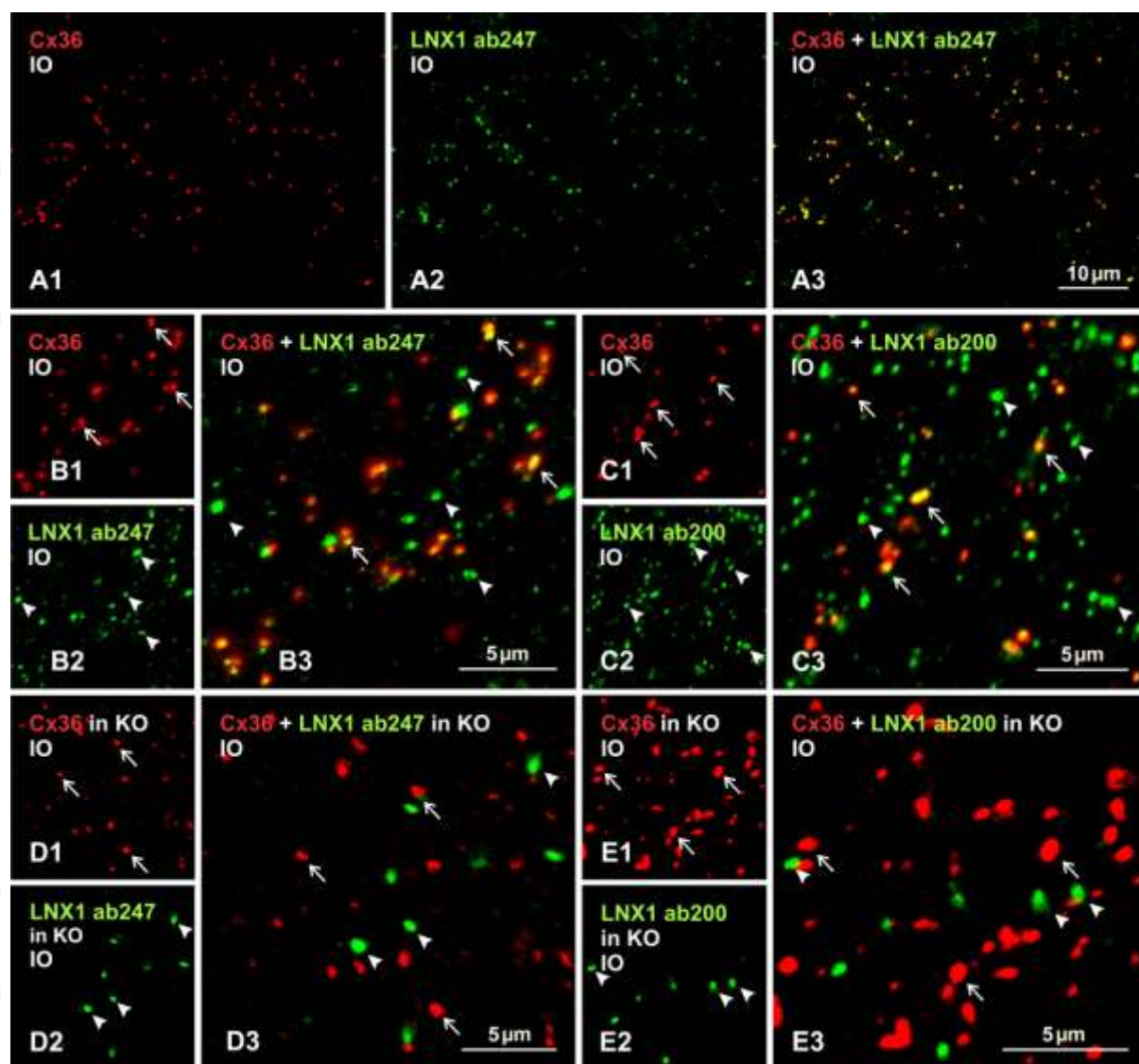
pull-downs (lanes 8, 9, 10 and 12). Lysates loaded in lanes 7 and 11 contain no His-tagged PDZ domain fusion protein.

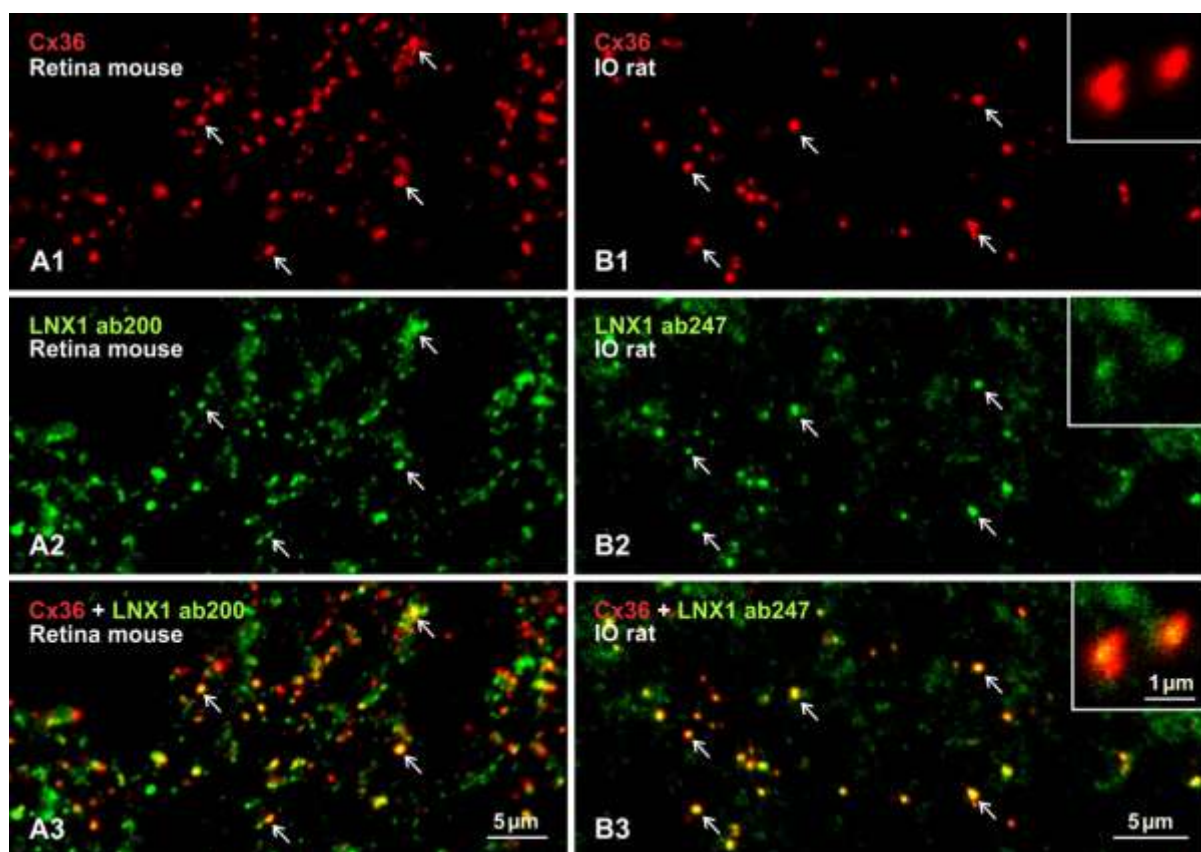
Fig. 8. Immunofluorescence localization of LNX proteins in Cx36-eCFP transfected N2A cells. (A) Cx36-eCFP fluorescence reveals large gap junctions at cell-cell contacts (arrows) and intracellular puncta (arrowheads). (B) Images of the same field of Cx36-eCFP-transfected cells, showing co-localization of Cx36-eCFP fluorescence (B1) and immunolabelling of Cx36 (B2) at gap junctions (arrows) and intracellular structures (arrowheads), as seen by yellow in image overlay (B3, arrows). (C) Four images of the same field of cells co-transfected with Cx36-eCFP and LNX1p70, showing Cx36-eCFP fluorescence (C1), labelling of Cx36 (C2) and labelling of LNX1 (C3) intracellularly (arrows) and at gap junctions (arrows), and co-localization as seen by yellow in image overlay (C4, arrows). (D) Three images of the same field of cells co-transfected with Cx36-eCFP and LNX1p80-FLAG, showing absence of Cx36-eCFP fluorescence (D1) and immunolabelling of Cx36 (D2) at cell contacts in cells immunolabelled for LNX1p80 (D3). (E) Cells transfected with LNX1p80-FLAG, showing co-distribution of immunolabelling with anti-FLAG (E1) and anti-LNX1 (E2). (F) Cells co-transfected with Cx36-eCFP (F1) and LNX2-FLAG (F2), showing absence of Cx36-eCFP at cell contacts. (G) Cells co-transfected with Cx36-eCFP and LNX2^{C51A}-FLAG, showing intracellular and gap junctional eCFP fluorescence (arrows), which is co-localized with immunolabelling with anti-FLAG (arrows).

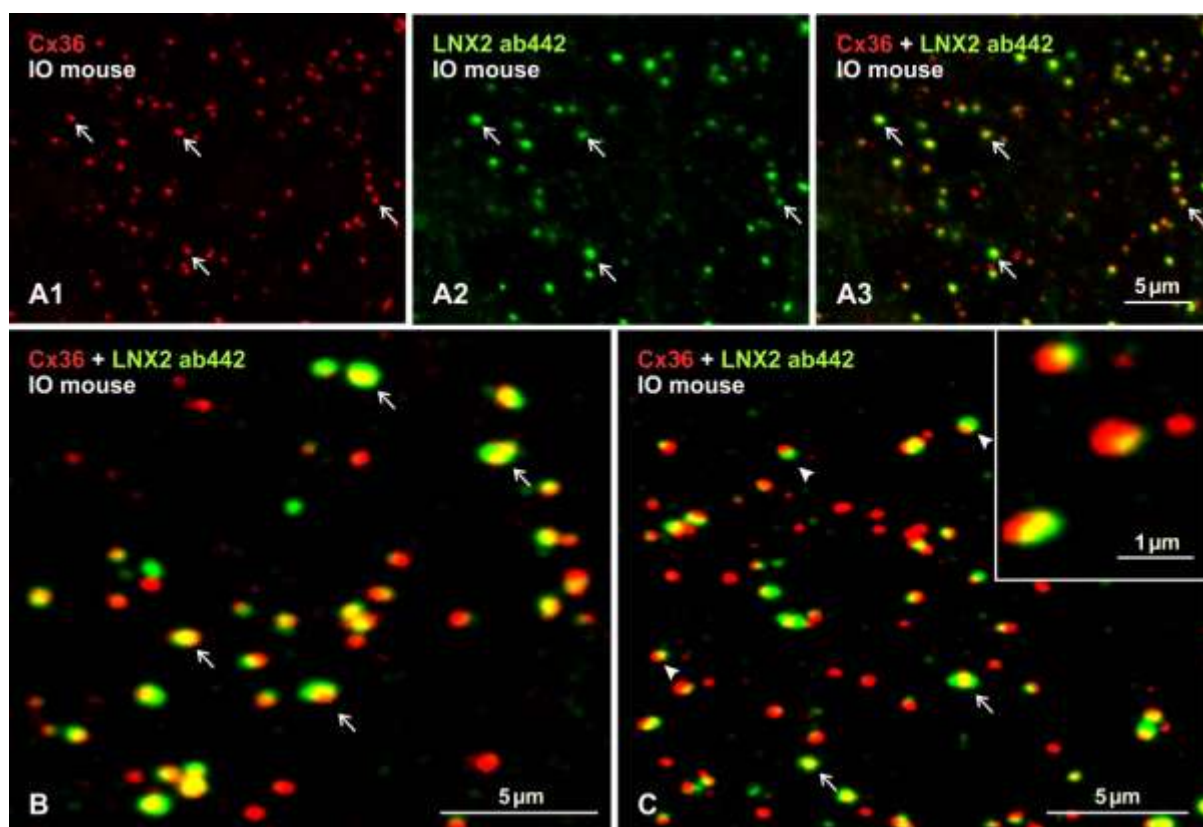
Fig. 9. Immunoblot showing requirement of functional LNX2 RING domain for LNX2-mediated ubiquitination of Cx36-eCFP. (A) IP of Cx36-eCFP with anti-eGFP from N2A cells co-transfected with Cx36-eCFP, HA-ubiquitin and either FLAG-vector, LNX2-FLAG or LNX2^{C51A}-FLAG. IP material was immunoblotted and probed with anti-HA. Low baseline levels of ubiquitinated Cx36-eCFP were detected in IPs of cells co-transfected with FLAG-vector (lane 1). An increase of HA-ubiquitinated Cx36-eCFP seen in IPs of cells co-transfected with LNX2-FLAG (lane 2) was not seen in IPs from cells co-transfected with mutant LNX2^{C51A}-FLAG (lane 3). Control IPs with normal rabbit IgG from lysates of cells co-transfected with LNX2-FLAG showed lack of detection of HA-ubiquitin (lane 4). (B) IgG heavy (IgG H-Chain) and light chains (IgG L-Chain) were revealed in images of TGX-stain-free SDS-PAGE gels used for immunoblot shown in (A), indicating the equivalent amounts of IgG used for each IP (lanes 1-4 in A). (C) Immunoblot of input cell lysates used for IPs shown in (A) probed with anti-FLAG, showing detection of LNX2-FLAG (lane 2) and

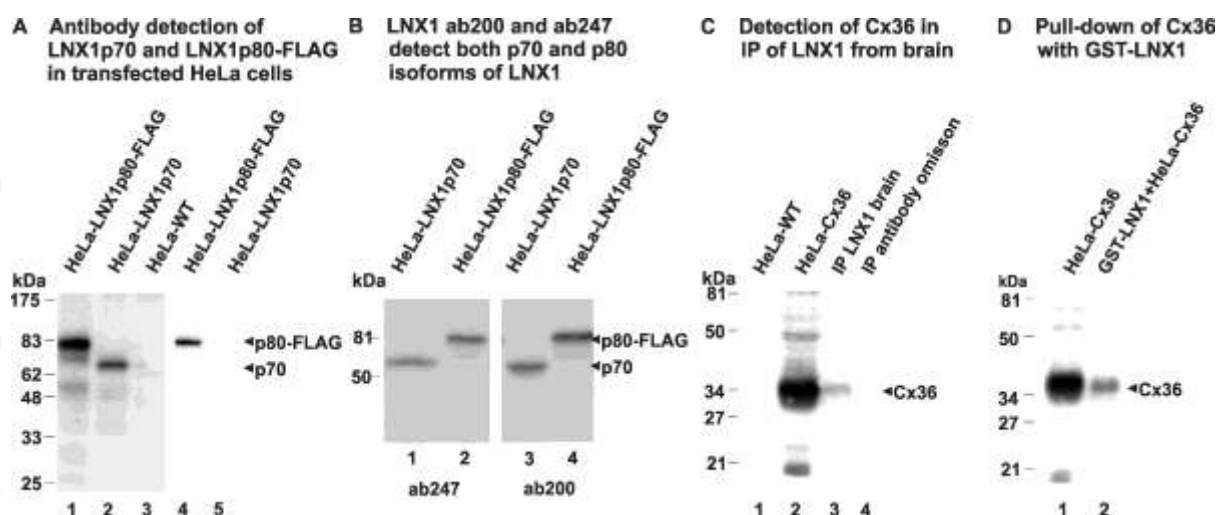
LNX2^{C51A}-FLAG (lane 3) in cells co-transfected with these constructs, and lack of FLAG detection in lysates from cells co-transfected with vector-FLAG (lane 1). (D) The blot in (C) was stripped and re-probed with anti-eGFP revealing decreased detection of Cx36-eCFP in lysates from cells co-transfected with LNX2 (lane 2) vs. those co-transfected with vector-FLAG (lane 1) or LNX2^{C51A}FLAG (lane 3). (E) Image of TGX-stain-free SDS-PAGE gel used to prepare immunoblots shown in C and D, indicating approximately equal protein sample loading.

Fig. 10. Immunoblot of lysates from N2A cells probed with anti-Cx36 after co-transfection with Cx36-eCFP and either FLAG-vector, or wild-type LNX2-FLAG or mutant LNX2^{C51A}-FLAG lacking its RING domain.. (A) Cells were treated with lysosome inhibitors chloroquine or ammonium chloride as indicated. Cells transfected with Cx36-eCFP and empty FLAG-vector displayed a band migrating at ~60 kDa (lane 1), corresponding to the molecular weight of Cx36 plus eCFP, which was only faintly detected in Cx36-eCFP cells co-expressing LNX2-FLAG (lane 2), but was present in cells co-expressing LNX2^{C51A}-FLAG (Lane 3). Detection of this band in cells expressing LNX2 was recovered after treatment with 10-100 mM chloroquine (CQ; lanes 4-6) or with 25 mM ammonium chloride (NH₄CL; lane 7). Negative control lane shows absence of Cx36-eCFP in lysate of N2A cells transfected with only FLAG-vector (lane 8). (B) The blot shown in (A) was stripped and re-probed with anti-FLAG, showing presence of LNX2-FLAG and LNX2^{C51A}-FLAG in correspondingly transfected cells (lanes 10-15), and its absence in cells not transfected with these constructs (lanes 9 and 16).



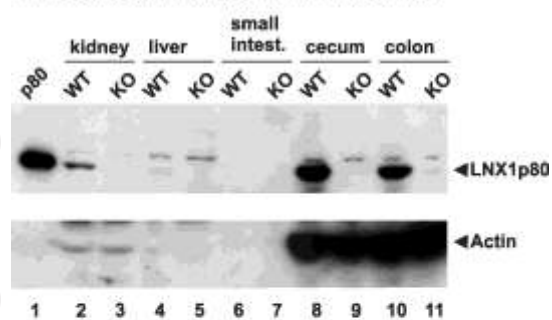




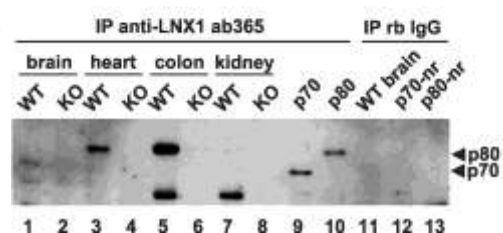


Accepted Article

A Absence of LNX1p80 in LNX1 KO mice

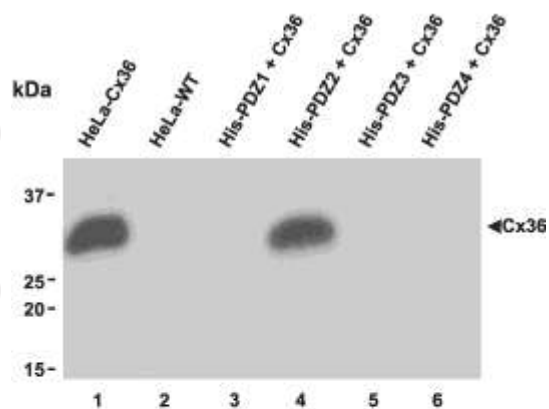


B IP of LNX1 from WT and KO tissues

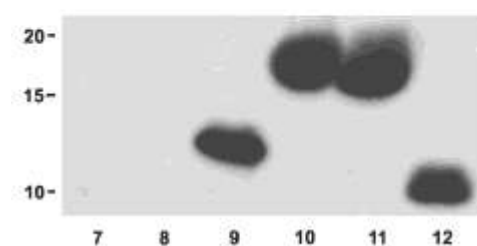


Accepted Article

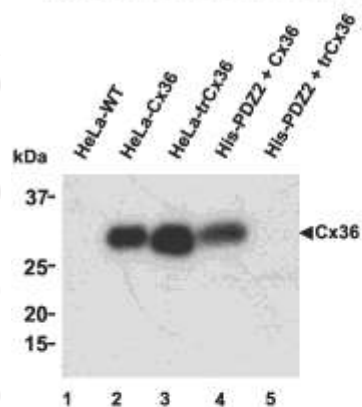
A Pull-down of Cx36 with PDZ domain 2 of LNX1



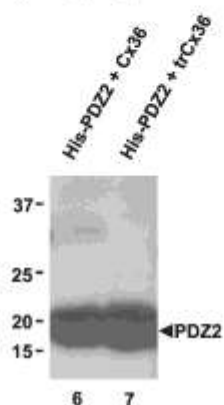
B



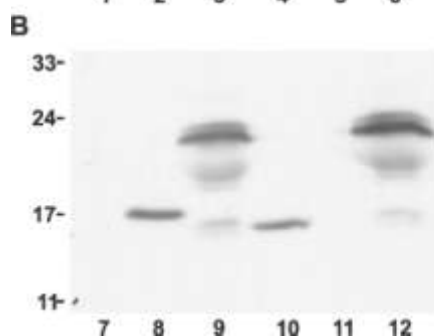
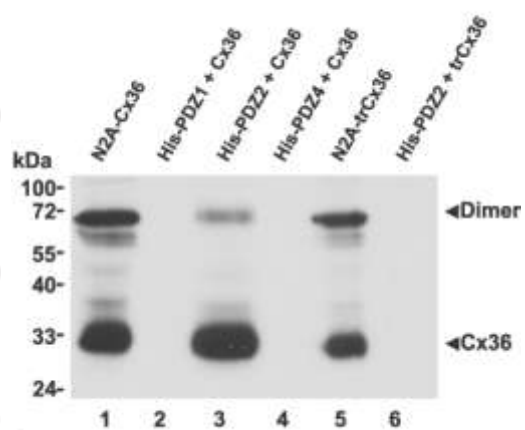
C Requirement of the PDZ ligand of Cx36 for interaction with PDZ domain 2 of LNX1

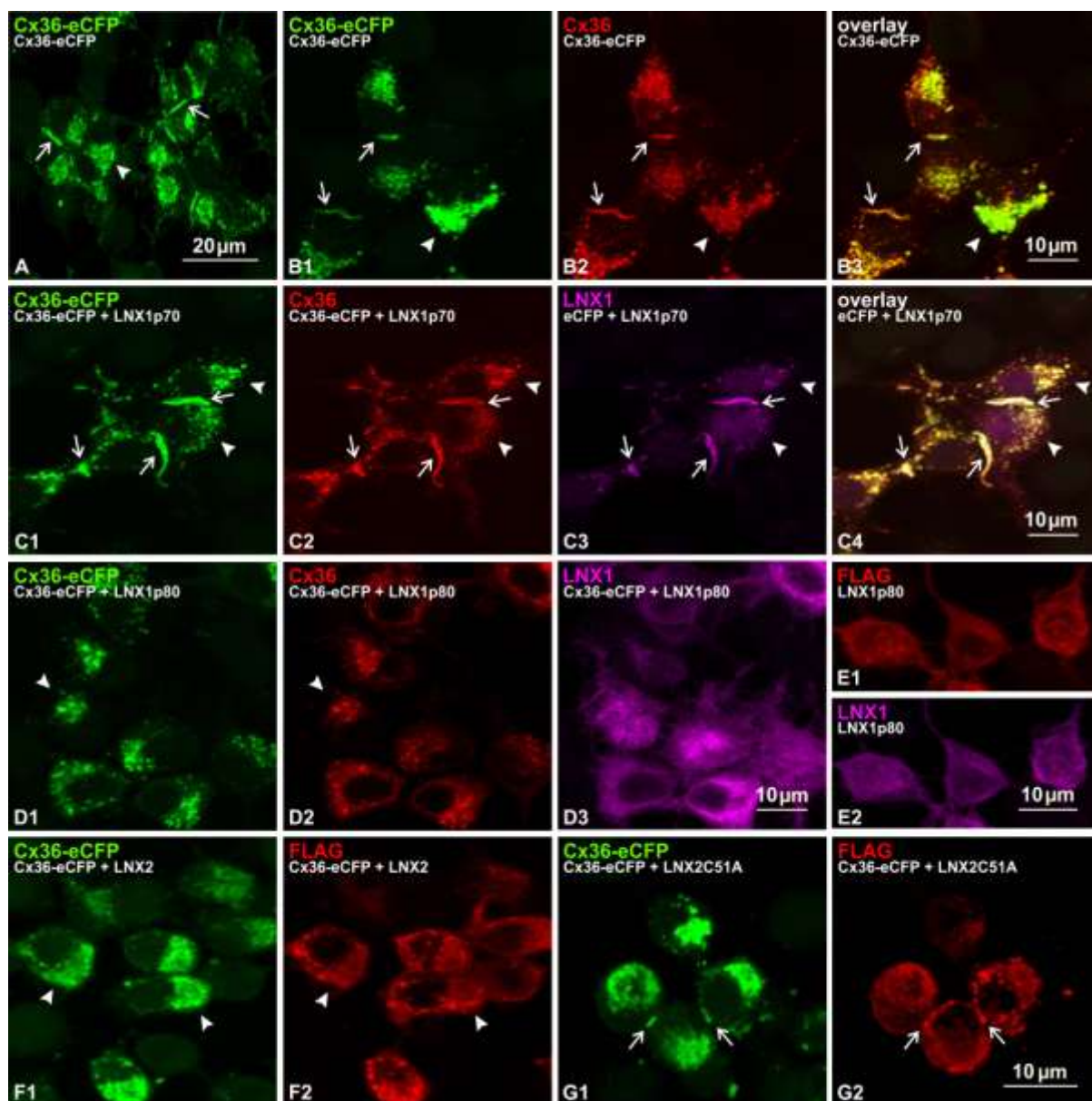


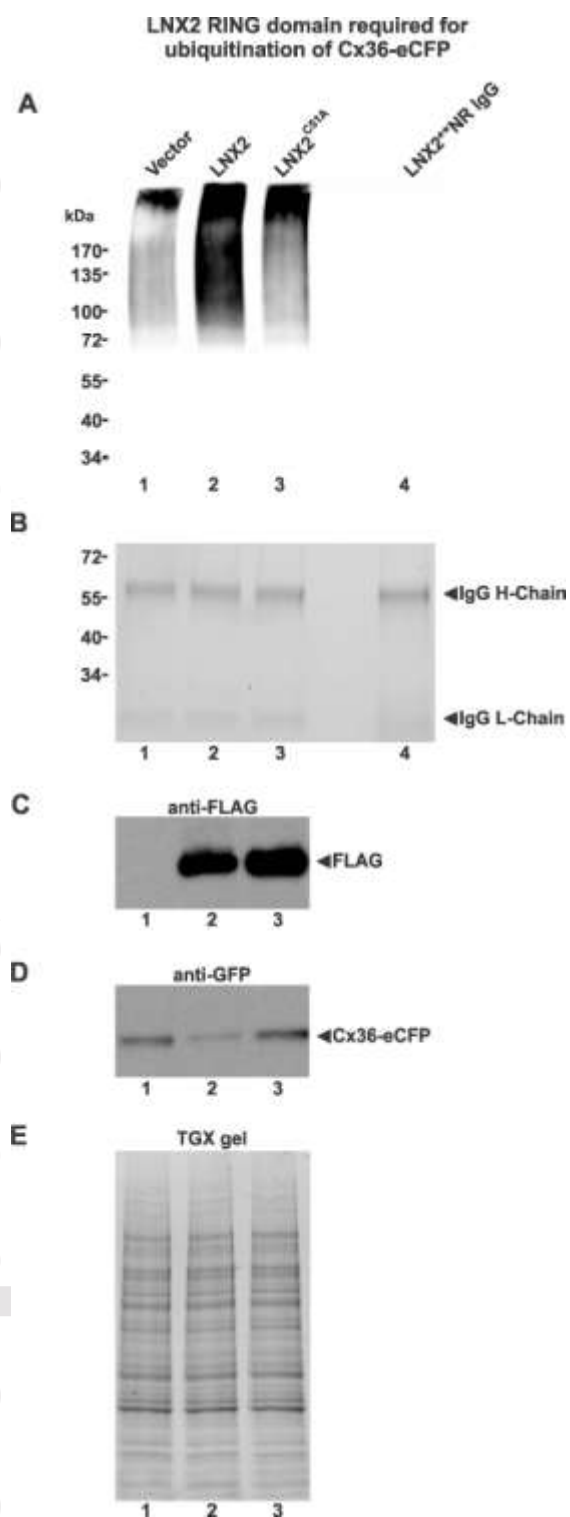
D



A Requirement of the PDZ ligand of Cx36 for interaction with PDZ domain 2 of LNX2

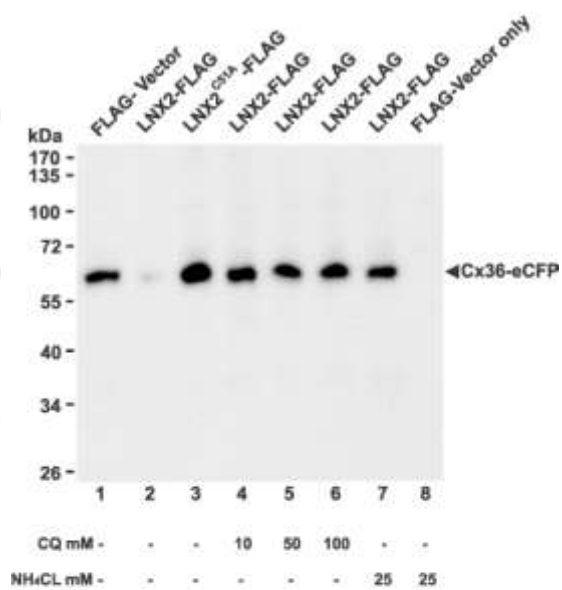






Accepted Article

A LNX2 promotes Cx36-eCFP degradation



B

